Theory of liquidstate activated barrier crossing: The instantaneous potential and the parabolic model

Steven A. Adelman and R. Muralidhar

Citation: The Journal of Chemical Physics **95**, 2752 (1991); doi: 10.1063/1.460927
View online: http://dx.doi.org/10.1063/1.460927
View Table of Contents: http://scitation.aip.org/content/aip/journal/jcp/95/4?ver=pdfcov
Published by the AIP Publishing

Theory of liquid-state activated barrier crossing: The instantaneous potential and the parabolic model

Steven A. Adelman
Department of Chemistry, Purdue University, West Lafayette, Indiana 47907

R. Muralidhar
School of Chemical Engineering, Purdue University, West Lafayette, Indiana 47907

(Received 26 January 1990; accepted 12 April 1991)

This paper gives a theoretical treatment of liquid-phase activated barrier crossing that is valid for chemical reactions which occur on typical (e.g., high activation barrier) potential-energy surfaces. This treatment is based on our general approach [S. A. Adelman, Adv. Chem. Phys. **53**, 61 (1983)] to problems in liquid-phase chemical dynamics. We focus on the early-time regime [times short compared to the relaxation time of $\langle \tilde{F}(t)\tilde{F}\rangle_0$, the fluctuating force autocorrelation function of the reaction coordinate] in which the solvent is nearly "frozen." This regime has been shown to be important for the determination of the rate constant in the molecular-dynamics simulations of model aqueous S_N2 reactions due to Wilson and coworkers. Our treatment is based on a generalized Langevin equation of motion which naturally represents the physics of the early-time regime. In this regime the main features of the reaction dynamics are governed by the instantaneous potential $W_{\rm IP}[y,\tilde{F}]$, which accounts for the cage confinement forces which dominate the liquid-phase effects at early times, rather than by the familiar potential of mean force. The instantaneous potential is derived from the $t\rightarrow 0$ limit of the equation of motion and its properties are developed for both symmetric and nonsymmetric reactions. The potential is then shown to account for both the early-time barrier recrossing processes found to determine the transmission coefficient κ in the S_N2 simulations and the dependence of these processes on environmental fluctuations modeled by $\tilde{F}$. Making the parabolic approximation for the gas-phase part of $W_{\rm IP}[y,\tilde{F}]$ yields the following result for the transmission coefficient:

$$\kappa = \omega_{\rm PMF}^{-1} x_+ = \omega_{\rm PMF}^{-1}\omega_{\rm MIP}\left[1+\omega_{\rm MIP}^{-2}\hat{\Theta}(x_+)\right]^{1/2} \doteq \omega_{\rm PMF}^{-1}\omega_{\rm MIP}\left[1+\tfrac{1}{2}\omega_{\rm MIP}^{-2}\hat{\Theta}(\omega_{\rm MIP})\right],$$

where $\omega_{\rm MIP}$ and $\omega_{\rm PMF}$ are, respectively, the barrier frequencies of $W_{\rm IP}[y,\tilde{F}=0]$ and of the potential of mean force, and where $\hat{\Theta}(x_+)=\int_0^\infty \exp(-x_+ t)\Theta(t)dt$ with $\Theta(t)\equiv(k_BT)^{-1}\langle\tilde{F}(t)\tilde{F}\rangle_0$. This result for κ, which is equivalent to a result of Grote and Hynes, but which more naturally represents the physics of the early-time regime, permits a straightforward interpretation of the variation of the transmission coefficients for the model S_N2 systems.

I. INTRODUCTION

In this paper we begin the development of a theory of the activated barrier crossing processes which occur during "typical" liquid-phase chemical reactions. An example of such a typical reaction is the aqueous $Cl^- + CH_3Cl$ nucleophilic substitution process. Reaction path potentials for the $Cl^- + CH_3Cl$ S_N2 system are plotted in Figs. 1 and 2. The theory initiated here is based on our general approach[1-7] to problems of chemical dynamics in liquid solution. The concepts underlying this approach are receiving increasing support from the results of molecular-dynamics (MD) simulations[8,9] and experiments.[10]

Specifically, we note that typical reactions occur on gas-phase potential-energy surfaces characterized by generic features,[11] e.g., high activation barriers for thermoneutral reactions, steep "cliffs" for strongly exothermic reactions, which can produce forces acting on the reaction coordinate of tremendous[12] accelerating power. A consequence of this type of force law is that the solvent cannot even approximately adiabatically readjust and thus remain in near thermodynamic equilibrium with the instantaneous solute configuration. Rather, the solvent following of the solute motions which occur during a typical chemical reaction is highly imperfect relative to its following of the more familiar[13] thermal liquid-phase motions. Thus forces which act to restore thermodynamic equilibrium play a critical role in influencing the reaction dynamics. These restoring forces, for example, lead to a special type of solute dynamics, often oscillatory,[8(a)] which can differ qualitatively from either thermal liquid-phase solute dynamics[13] or gas-phase reaction dynamics. It is important to note that the nonequilibrium restoring forces are *not* properly described in traditional theories of liquid-phase activated barrier crossing, e.g., the transition-state[11,14] or Kramers[15] theories. This is because these traditional descriptions are based on the equilibrium potential, i.e., the potential of mean force (Fig. 1), and thus implicitly require that the solution remains close to thermo-

 0021-9606/91/162752-22$03.00

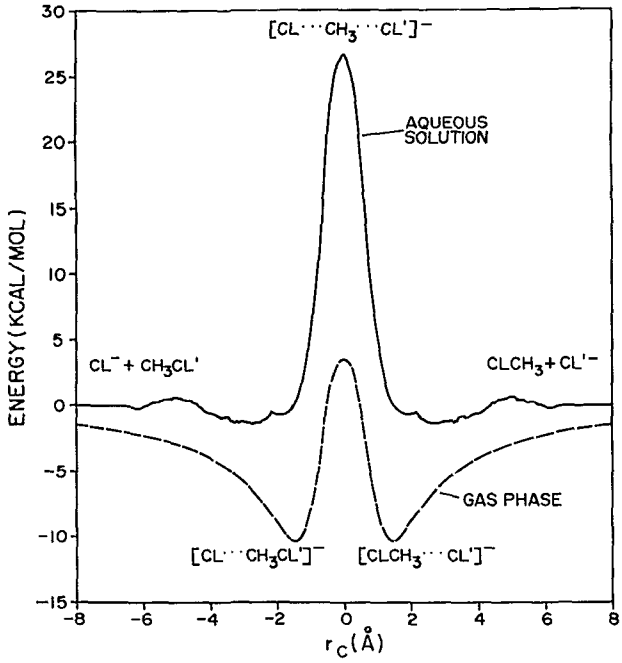

FIG. 1. Reaction-path potentials for the aqueous $Cl^- + CH_3Cl'$ S_N2 system near standard conditions. The gas-phase potential and the potential of mean force, computed in Ref. 17, are plotted vs $r_c = r_{CCl'} - r_{CCl}$.

dynamic equilibrium during the course of a reactive event.

In this paper we develop the implications of these concepts for the special case of reaction coordinate motion occurring in the *early-time regime* [time scales short compared to the relaxation time of the fluctuating force autocorrelation function $\langle \tilde{F}(t)\tilde{F}\rangle_0$ of the reaction coordinate]. Barrier recrossing processes[1(d),3] occurring in this time-scale regime were shown to determine the transmission coefficient $\kappa = k/k_{TST}$ for model aqueous thermoneutral S_N2 reactions, including the $Cl^- + CH_3Cl$ reaction, in recent MD simulations due to Wilson and co-workers.[8]

In the early-time regime, the solvent remains nearly "frozen"[16] at its initial configuration and the main features of the reaction dynamics are governed by the *instantaneous potential*, introduced in Sec. III, rather than by the familiar potential of mean force. The instantaneous potential is the potential which would exactly govern the dynamics if the time required for the reactive event were infinitely short. It is a superposition of the gas-phase potential and the *cage potential*. The cage potential determines the restoring forces exerted by the "frozen solvent" on the reaction coordinate. The most probable instantaneous potential $W_{MIP}[y]$ (see Sec. III D) is plotted for the aqueous $Cl^- + CH_3Cl$ system in Fig. 2. Notice that $W_{MIP}[y]$ differs qualitatively from the potential of mean force $W_{PMF}[y]$, computed for the same system by Chandrasekar and co-workers[17] and plotted in Fig. 1.

The physics of imperfect following may be described very simply in the early-time regime. In zeroth order the reaction coordinate moves in the instantaneous potential produced by the frozen solvent. In first order this zeroth-order conservative description is modified by energy dissipation due to weak environmental relaxation possible because of the finite time of the displacement. This physics reflects itself in a formula for the transmission coefficient κ, developed later in the paper, which is valid within the parabolic model (see Fig. 2) for $W_{MIP}[y]$. This result for κ takes the form

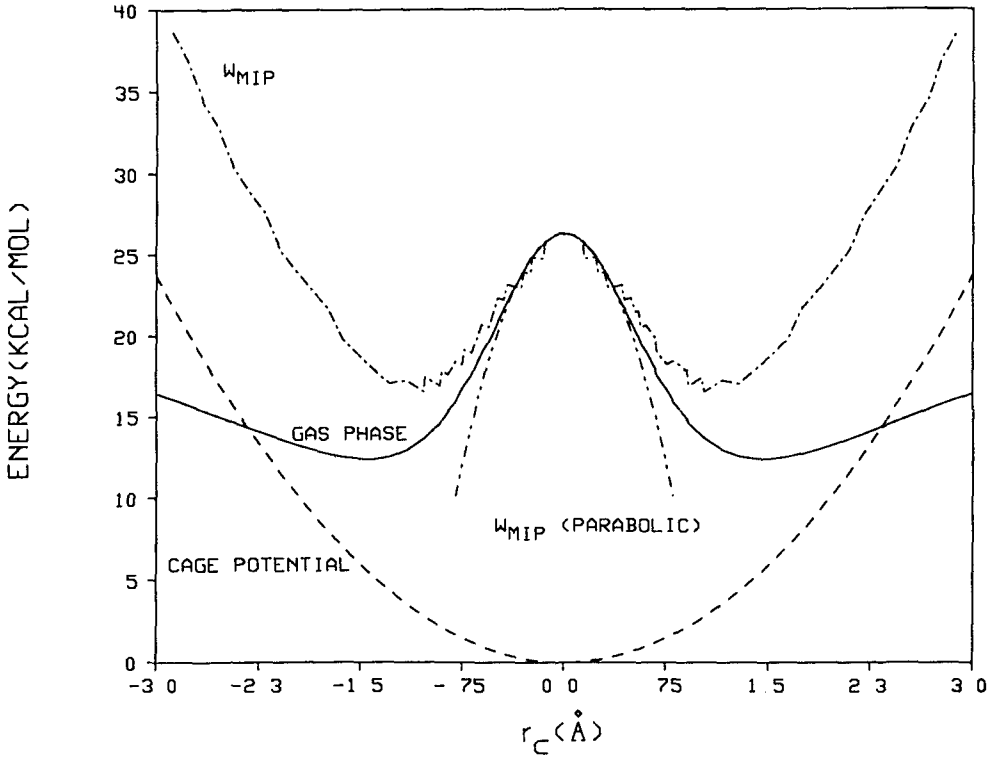

FIG. 2. Reaction-path potentials for the aqueous $Cl^- + CH_3Cl$ S_N2 system near standard conditions. The instantaneous potential, computed from Eq. (4.9) for a "symmetric environment" (fluctuating force $\tilde{F} = 0$), is plotted vs r_c. The gas-phase potential used in this computation is from Ref. 17. The liquid-phase contributions are estimated (see Sec. IV C) from the data of Ref. 8. Replacing the gas-phase potential by a parabolic barrier with frequency $\omega_g = 461\ cm^{-1}$, obtained from Ref. 8(a), yields the plotted parabolic approximation. Note that the wings of W_{MIP} are only of qualitative significance since the harmonic cage potential model is invalid for large r_c.

$$\kappa = \omega_{\mathrm{PMF}}^{-1} x_+ , \tag{1.1}$$

where ω_{PMF} is the parabolic barrier frequency of the potential of mean force and where the reactive frequency x_+ is defined by the following self-consistent equation,

$$x_+ = \omega_{\mathrm{MIP}} [1 + \omega_{\mathrm{MIP}}^{-2} \hat{\Theta}(x_+)]^{1/2}. \tag{1.2}$$

In the above equation, ω_{MIP} is the parabolic barrier frequency of $W_{\mathrm{MIP}}[y]$ and the relaxation function $\hat{\Theta}(x_+)$ is given by the Laplace transform relation

$$\hat{\Theta}[x_+] = \int_0^\infty \exp(-x_+ t)\Theta(t)dt, \tag{1.3}$$

where $\Theta(t) \equiv (k_B T)^{-1} \langle \tilde{F}(t)\dot{\tilde{F}} \rangle_0$.

Equations (1.1)–(1.3) for κ are equivalent to a result of Grote and Hynes[18] but more naturally represent the physics of the early-time regime. This may be seen by specializing to the weak response limit $\omega_{\mathrm{MIP}}^{-2} \hat{\Theta}(x_+) \ll 1$. Equations (1.1) and (1.2) then yield the following approximate result for κ:

$$\kappa \doteq \omega_{\mathrm{PMF}}^{-1} \omega_{\mathrm{MIP}} [1 + \tfrac{1}{2} \omega_{\mathrm{MIP}}^{-2} \hat{\Theta}(\omega_{\mathrm{MIP}})]. \tag{1.4}$$

Equation (1.4) describes κ as a superposition of the frozen solvent result $\kappa_0 = \omega_{\mathrm{PMF}}^{-1} \omega_{\mathrm{MIP}}$ (first derived by van der Zwan and Hynes[19]) and a correction, $(1/2)(\omega_{\mathrm{PMF}}\omega_{\mathrm{MIP}})^{-1}\hat{\Theta}(\omega_{\mathrm{MIP}})$, which accounts for the weak environmental relaxation. Equation (1.4) is at this stage a conceptualization of the relaxation process. It is of interest since it shows that κ can be expressed in a form which clearly reflects the underlying physics of a nearly frozen solvent. We hope to quantitatively assess Eq. (1.4) for specific systems in the future.

We next indicate some connections between the present work and the related work of others. We emphasize, in particular, the gradual development of the concept of the instantaneous potential.

Some of the earliest related discussions appeared in the 1960s in papers on proton transfer kinetics.[16] The first discussions were qualitative. Grunwald and Price,[16a] for example, argued that "the mean time for the transition between the initial state and the transition state" for at least some proton transfer processes is "probably less than τ_D"—the dielectric relaxation time of the solvent. As a consequence, "the permanent dipoles of the solvent molecules do not have time to come into equilibrium with the changing charge distribution of the reacting system and the solvent polarization due to orientation is essentially constant." Grunwald and Price[16(a)] then qualitatively discussed proton transfer energetics using these concepts of "nonequilibrium solvation." Similar qualitative discussions of proton transfer kinetics were given by Bell,[16(a)] Williams and Kreevoy,[16(a)] and others.

Kurz and Kurz[16(b)] gave an early quantitative treatment of proton transfer kinetics in the frozen-solvent limit. Kurz and Kurz[16(b)] made an approximate calculation of the cage potential in which the frequency associated with its well curvature, the Einstein frequency ω_e of our theory,[1-7] is approximated by the frequency associated with the free energy required to create a small solvent fluctuation. This latter frequency is computed assuming a continuum electrostatic model to yield an estimate of the cage potential and the frozen-solvent potential.

Similar ideas were discussed by van der Zwan and Hynes,[19] who considered more general problems of charge transfer and dipolar rearrangement in polar solvents. For example, in Ref. 19(a), they idealize "the reactive event as a passage of a charge (or dipole) over a parabolic chemical barrier, whose fixed frequency is ω_b." Furthermore, they use a "primitive continuum model" for the solvent. They compute the friction kernel $\zeta_D(t)$ of the reaction coordinate using a "direct time-dependent generalization" of the continuum model of Kurz and Kurz[16(b)] and find an "approximately exponential" decay with time constant of the order of the longitudinal dielectric relaxation time of the solvent. They compute a frequency ω_s, which determines the well curvature of the cage potential, from the relation $\omega_s^2 = \zeta_D(t=0)$. By superimposing their cage potential with their parabolic barrier potential, they obtain a fluctuationless frozen-solvent potential. The parabolic fit to the maximum of our $W_{\mathrm{MIP}}[y]$ is identical to their frozen-solvent potential.

Bergsma *et al.*[8(a)] [also see discussion in Ref. 8(c)] introduced a "frozen-solvent nonadiabatic solvation model" [See Sec. III B 3 of Ref. 8(a)], which formulates the frozen-solvent potential in terms of quantities which involve the instantaneous solvent configuration and which, therefore, incorporates the effects of solvent fluctuations. To obtain this potential, the reaction coordinate potential, $V_T(R)$ in their notation, is expanded about its transition-state value $R = 0$ to quadratic order in R to yield [see Eqs. (3.10)–(3.13) of Ref. 8(a)]

$$V_{\mathrm{eff}}(R) \equiv V_T(R) - V_T(R=0)$$

$$= -RF_s - \frac{1}{2}\mu\omega_{b,na}^2 R^2, \tag{1.5}$$

with

$$\omega_{b,na}^2 = \omega_b^2 - (\Delta\omega)^2, \tag{1.6}$$

where ω_b^2 is the square of the gas-phase barrier frequency (ω_g^2 in our notation) and the liquid-phase contribution to $\omega_{b,na}^2$ is the squared "solvent bias frequency" $(\Delta\omega)^2$. Both F_S and $(\Delta\omega)^2$ include the effects of solvent fluctuations. Bergsma *et al.*[8(a)] give the following physical interpretations of the quantities appearing in Eq. (1.5). The "solvent bias frequency reflects a shift in the barrier curvature, while the solvent bias force F_s shifts the barrier position (and ... its energy)." Bergsma *et al.*[8(a)] recast Eq. (1.5) in the following form:

$$V_{\mathrm{eff}}(R) = -\frac{1}{2}\mu\omega_{b,na}^2\left(R + \frac{F_s}{\mu\omega_{b,na}^2}\right)^2 + \frac{F_s^2}{2\mu\omega_{b,na}^2}, \tag{1.7}$$

which shows shifts $\Delta R = F_s/\mu\omega_{b,na}^2$ and $\Delta V = F_s/2\mu\omega_{b,na}^2$ in, respectively, the "location of the instantaneous solvent transition barrier" and in the potential energy, due to solvent fluctuations. The shift in the barrier position ΔR is correlated by Bergsma *et al.* with the solvent configuration depen-

dence of barrier recrossing probabilities observed in their S_N2 simulations.[8(a)]

Our work in this paper emerged from a quite independent line of development which began in 1979.[1(b)] The central idea behind the development is the importance of the short-time-scale limit of the full many-body problem for *general* chemical processes (as opposed to, say, proton transfer processes[16]) in condensed phases. This limit, which is referred to as the "Einstein limit" in early papers[1(a),1(b)] is identical to the frozen-solvent limit.[8,16,19] The imperfect following concept introduced here is a natural generalization of our early[1(a)] Einstein-limit concept.

Given currently available methods for treating irreversible processes, the best way to formulate the physics emphasized here is via generalized Langevin equations. At the core of our theory is a rigorous formulation of generalized Langevin equations of motion [see, especially, the equivalent chain equations of Ref. 1(a)] which bring out the physics of imperfect following. Our equations of motion emphasize the Einstein frequency ω_e while the conventional Mori equations emphasize the adiabatic frequency Ω_0. The Einstein frequency determines the well curvature of the cage potential while the adiabatic frequency determines the well curvature of the liquid-phase contribution to the potential of mean force.

Our exact formalism for short-time-scale irreversible dynamics[1(a)] was developed into an approximate theory[1(d),1(e),2-7] of liquid-phase chemical-reaction dynamics which will be briefly discussed here. Our work in this paper is based on the partial-clamping equation,[5] an approximate generalized Langevin equation of motion for those solute generalized coordinates (e.g., the reaction coordinate) whose dynamics controls the process of interest. This equation of motion can be solved analytically in special cases to obtain rate-constant expressions; see, e.g., Eqs. (1.1) and (1.2). The quantities appearing in the partial-clamping equation, and hence the rate-constant formulas, can be explicitly evaluated for specific systems (see Refs. 6 for an application to solute vibrational energy relaxation) in terms of solute–solvent site–site potential-energy and equilibrium pair-correlation functions. Specifically: (i) the Einstein frequency ω_e can be constructed directly since it is an equilibrium property. (ii) The friction kernel can be constructed in terms of equilibrium properties within the Gaussian model.[6] The Gaussian-model friction kernel, which has a qualitatively different form than the nearly exponential form found by van der Zwan and Hynes,[19] has been shown [see, e.g., the discussion in Ref. 6(b)] to provide a realistic description of solvent dynamics for many Lennard-Jones systems in the short-time regime important for reaction dynamics. (iii) The probability distribution function (PDF) for the fluctuating force may be constructed from equilibrium properties within the Gaussian noise model. The PDF for the initial value of the fluctuating force $\tilde{F}$, for example, is determined by the equilibrium property $\langle \tilde{F}^2 \rangle_0$.

Our work in this paper is, in essence, a recasting of the work in Refs. 1–7 into the frozen-solvent potential language of Refs. 8, 16, and 19. This is easily accomplished by taking the $t \to 0$ limit of the partial-clamping equation of motion. The potential-energy function which corresponds to the force term in the limiting equation is our frozen-solvent potential, the instantaneous potential. The parabolic model limit of the instantaneous potential formally resembles the frozen-solvent potential, Eq. (1.5), of Bergsma *et al.*[8(a)] This is because the quadratic order expansion of Eq. (1.5) is equivalent to the small-amplitude excursion approximation inherent in our full-clamping[1(a)] and partial-clamping[5] treatments. For example, the ensemble average of their squared solvent bias frequency is the square of our Einstein frequency.

The present treatment is aimed at a general formulation of the instantaneous potential designed to set it on approximately the same footing as the potential of mean force. (However, unlike the potential of mean force, the instantaneous potential depends on the initial equilibrated solvent configuration.) Thus our treatment differs from and goes beyond the model of Bergsma *et al.*[8(a)] (i) We base our treatment on a realistic, rather than a parabolic model, reaction coordinate potential. Preliminary calculations[7(b),18] have shown that the parabolic model can break down qualitatively for strongly nonthermoneutral reactions. (ii) We use the generalized Langevin decomposition of the total force into systematic and random components. This permits explicit construction of the instantaneous potential for specific systems via the procedures[6] described above. For example, the curvature of the cage potential may be evaluated since it depends on the equilibrium property ω_e while the PDF which governs the range of values its minimum can take (analogous to the shifts ΔR of Bergsma *et al.*[8(a)]) may be estimated, using the Gaussian noise model, from the equilibrium property $\langle \tilde{F}^2 \rangle_0$. (iii) We decompose the total frozen-solvent potential into gas-phase and cage-potential contributions. Making this decomposition gives, especially for nonsymmetric reactions, a clearer picture of the solvent effect in the early-time regime (see Secs. III I and III J). (iv) We give a consistent treatment of the work required to create a solvent fluctuation. This treatment gives a picture of the energetics of activation in the presence of fluctuations which is very different from that of Bergsma *et al.*[8(a)] (v) Points (iii) and (iv) allow us to develop the "coupled-oscillator" mathematical structure of the instantaneous potential.

Finally, we note that Gertner, Wilson, and Hynes[8(b)] have derived a result for the parabolic model transmission coefficient [Eqs. (2.16) and 2.17) of Ref. 8(b)] which expresses κ as a *linear superposition* of the frozen-solvent result κ_0 (Ref. 19) and a correction. This result differs in form from our *nonlinear* equations (1.1) and (1.2), and the dependence of κ on the relaxation function $\Theta(x_+)$ is not immediately evident from the result of Ref. 8(b).

The plan of this paper is as follows. In Sec. II the equation of motion for the reaction coordinate, which is the basis of the work in the remainder of this paper, is presented and described. In Sec. III, the form of the instantaneous potential is developed, and its properties are worked out for both symmetric and nonsymmetric reactions in Sec. III. A comparison of the instantaneous potential and the potential of mean force is also given in Sec. III. In Sec. IV those aspects of the computational studies of the aqueous $Cl^- + CH_3Cl$ S_N2

reaction due to Chandrasekhar and co-workers[17] and Wilson and co-workers[8] relevant to the present work are summarized. These computational results are utilized in the applications of the theory given in Sec. III I.

Section V and Appendixes A and B are concerned with the development and application of the parabolic model transmission coefficient formula given in Eqs. (1.1)–(1.3). In particular, in Sec. V C we apply our result for κ to interpret the variation of the transmission coefficients computed by Wilson and co-workers[8] for their model S_N2 systems. We close the paper in Sec. VI with a discussion and summary.

II. THE EQUATION OF MOTION

In this section, we introduce the equation of motion for reaction coordinate dynamics which is the basis of the work in the remainder of this paper. The plan of the section is as follows. A preliminary discussion of the liquid-phase reaction coordinate of the solute system is given in Sec. II A. The equation of motion is described in Sec. II B. An approximate form of the equation of motion, which will simplify the work in later sections, is described in Sec. II C.

A. The liquid-phase reaction coordinate

In this part, we introduce the definition, Eq. (2.5), of the reaction coordinate used in the remainder of this paper. We also discuss the choice of the liquid-phase transition state (TS) of the solute system and point out some difficulties associated with the specification of its liquid-phase reaction path.

We begin by defining the reaction coordinate as a generalized coordinate of a reactive molecular system whose value uniquely specifies a point on the minimum-energy reaction path (MERP) (path of steepest ascent and descent) of a suitably defined potential-energy surface of the system. That is, a one-to-one association exists between values of the reaction coordinate and MERP geometries.

The arc length s along the MERP, with $s = 0$ specifying the TS of the system, is the conventional choice of the reaction coordinate. Instead, we use here an alternative choice due to Chandrasekhar and co-workers[17] and Wilson and co-workers.[8]

Chandrasekhar and co-workers[17] have pointed out that for $A + BC \rightarrow AB + C$ atom transfer reactions the generalized coordinate,

$$r_c \equiv r_{BC} - r_{BA}, \tag{2.1}$$

where $r_{BA(C)}$ is the $BA(C)$ internuclear separation, satisfies the above criterion for a reaction coordinate. Gertner, Wilson, and Hynes[8(b)] alternatively choose the reaction coordinate to be the asymmetric stretch coordinate r_{as} of the ABC system which is defined in terms of r_c by[20]

$$r_{as} = +\tfrac{1}{2}r_c. \tag{2.2}$$

They then define a mass-weighted reaction coordinate x by

$$x = (\mu_{as})^{1/2} r_{as}, \tag{2.3}$$

where μ_{as} is the reduced mass factor associated with the asymmetric stretch coordinate r_{as}. In the applications presented in later sections of this paper we will restrict ourselves to *symmetric* reactions, i.e., reactions for which atoms A and C are identical. For such reactions, Gertner, Wilson, and Hynes[8(b)] give the following result for the mass factor μ_{as}:

$$\mu_{as} = \frac{2M_A M_B}{2M_A + M_B}\left[1 + \frac{M_A}{M_B}\left(1 + \frac{\mathbf{r}_{BA}\cdot\mathbf{r}_{BC}}{r_{BA}r_{BC}}\right)\right], \tag{2.4}$$

where $\mathbf{r}_{BA(C)} = \mathbf{r}_{A(C)} - \mathbf{r}_B$ and $M_{A(B)}$ equals the mass of $A(B)$.

We will, henceforth, assume that the reactive system is present at infinite dilution in a dense fluid solvent with Kelvin temperature T and number density ρ. We will, therefore, subsequently refer to the $A + BC$ system as the solute. To discuss activated barrier crossing of the solute, we must make a suitable choice for its *liquid-phase* transition state. We will choose this TS to be the saddle point of the potential of mean force surface of the solute. We will denote the value of the reaction coordinate at this saddle point by $x^\ddagger$. The motivation for this choice of liquid-phase TS will be discussed momentarily.

We will be concerned with the equilibrium rate constant of the solute. This may be computed[8,21] as a canonical ensemble average over all trajectories of the liquid solution for which the reaction coordinate initially has its TS value $x^\ddagger$. For this reason, in this paper we will choose the displacement y, defined by

$$y \equiv x - x^\ddagger, \tag{2.5}$$

as the reaction coordinate. The liquid-phase TS value of y will be denoted by $y^\ddagger$. Notice that $y^\ddagger = 0$.

We next discuss our motivation for choosing the saddle point of the potential of mean force surface as the liquid-phase TS. As mentioned, our main concern in the present paper is with the *equilibrium* rate constant of the solute. This rate constant may be constructed from the canonical ensemble average reactive flux through a dividing surface of the solute configuration space characterized by a fixed value of the reaction coordinate y^*.[22] The choice of y^* is, in principle, arbitrary. However, it is convenient to choose y^* so that the assumptions of transition-state theory[22] are well satisfied at $y = y^*$.[23]

Our choice $y^* = y^\ddagger$ is made in analogy to the conventional[22] choice of the gas-phase TS as the saddle point of the gas-phase potential-energy surface. This is the point of minimum canonical ensemble probability of the reactive system (conditional that the vibrational degrees of freedom of the solute are fixed at their equilibrium positions), and thus provides the natural transition point for the reaction in the absence of dynamical "bottlenecks."[23]

Similarly, in the liquid (once a canonical ensemble average over solvent phase-space coordinates has been performed), the saddle point of the potential of mean force surface is the point of minimum canonical ensemble probability and thus is a natural choice for the liquid-phase TS.

One additional point must be dealt with before conclud-

ing this discussion of the liquid-phase reaction coordinate. Namely, Eqs. (2.1)–(2.5) do not *fully define* the reaction coordinate. To make such a full definition one must specify a zeroth-order[24] *liquid-phase* potential-energy surface. Once this specification has been made Eqs. (2.1)–(2.5) permit a unique association of reaction coordinate values and MERP geometries on that surface, thus fully defining the reaction coordinate.

The most obvious choice of the liquid-phase potential-energy surface is the potential of mean force surface. While this choice appears to be satisfactory in the immediate neighborhood of the TS (see Sec. III E), for reasons discussed in the Introduction, a global identification of the liquid-phase potential surface with the potential of mean force surface is unsatisfactory. Thus there is ambiguity in the choice of the liquid-phase potential-energy surface. This ambiguity in the potential surface, in turn, implies a corresponding ambiguity in the definition of the liquid-phase reaction coordinate y.

These difficulties in the definition of the reaction coordinate y appear to complicate the problem of formulating a molecularly based equation of motion for y and hence a molecular theory of the rate constant. Fortunately, within the partial-clamping model developed by us elsewhere,[5] the complications may, to a considerable extent, be bypassed.

We next discuss the molecular equation of motion for y and briefly summarize the partial-clamping model upon which it is based.

B. Generalized Langevin equation of motion

The following generalized Langevin equation of motion for the reaction coordinate y may be derived[25] within the partial-clamping model [$\beta = (k_B T)^{-1}$],

$$\ddot{y}(t) = F_{\mathrm{MIP}}[y(t)] + \beta \int_0^t \langle \tilde{F}(t-\tau)\dot{\tilde{F}}\rangle_0 y(\tau)d\tau + \tilde{F}_{0(t)}(t), \tag{2.6a}$$

where the fluctuating force $\tilde{F}_{0(t)}(t)$ is given by

$$\tilde{F}_{0(t)}(t) = F_0(t) - \langle F\rangle_0 + \left[\frac{\partial F_0(t)}{\partial y^\ddagger} - \left\langle\frac{\partial F}{\partial y}\right\rangle_0\right] y(t). \tag{2.6b}$$

The precise mathematical definitions of all quantities appearing in the equation of motion (including a description of the notation), the physical assumptions underlying its derivation, and methods for its explicit construction for particular solute–solvent systems have been given elsewhere.[5,6] Therefore we will restrict ourselves here to a brief summary.

All quantities appearing in Eqs. (2.6) refer to the partial-clamping constraint. Namely, the reaction coordinate y is fixed at its *liquid-phase* TS value $y^\ddagger = 0$ while all other solute z and solvent q coordinates are allowed to move freely subject to this single constraint. Thus, e.g., $F_0(t)$ is the generalized force exerted by the solvent on the reaction coordinate y conditional that y is fixed at $y^\ddagger$; the symbol $\langle\cdots\rangle_0$ describes a canonical ensemble average over the phase-space coordinates of all solution degrees of freedom zq except y subject to the same constraint; $\langle\tilde{F}(t)\tilde{F}\rangle_0$ is the autocorrelation function of $\tilde{F}_0(t) \equiv F_0(t) - \langle F\rangle_0$, etc.

In particular, the generalized force $F_{\mathrm{MIP}}[y]$ appearing in Eq. (2.6a) is defined by

$$F_{\mathrm{MIP}}[y] = F_g[y] + \langle F\rangle_0 + \left\langle\frac{\partial F}{\partial y}\right\rangle_0 y, \tag{2.7}$$

where $F_g[y]$ is the gas-phase contribution to $F_{\mathrm{MIP}}[y]$, while $\langle F\rangle_0 + \langle\partial F/\partial y\rangle_0 y$ is the liquid-phase contribution to the linear order in y which is consistent with the small excursion assumption (see below) of the partial-clamping model.

We note that Gertner, Wilson, and Hynes[8(b)] have recently introduced a model which they call the "fixed-particle approximation," which they state is based on a small-amplitude excursion approximation. The fixed-particle approximation appears to be very similar or even identical to our[5] partial-clamping model, and so we will use the latter terminology in this paper.

We next briefly describe how Eqs. (2.6) may be constructed for particular solute–solvent systems. Equation (2.6) may be constructed either "exactly" via constrained molecular-dynamics (MD) simulations[6,8] or approximately and analytically[6] as indicated in the Introduction via a prescription based on integral equations for atomic[26] and molecular liquids.[27] (Huston, Rossky, and Zichi[6(d)] have developed an interesting alternative integral equation method and applied it to compute the frozen-solvent limit transmission coefficient κ_0 for aqueous S_N2 reactions. They utilize a "charging process" which bypasses the superposition approximation used in our method.) The MD construction for symmetric $A + BC$ reactions is particularly simple. For such reactions, the partial-clamping model may be implemented simply by constraining the AB and BC bondlengths to be identical. Such a MD implementation was recently performed by Wilson and co-workers[8(b)] for a set of model thermoneutral S_N2 reactions. Their results will be discussed in later sections.

We next discuss the most important physical assumption underlying the partial-clamping model, namely that on the time scales necessary to determine the rate constant, the reaction coordinate y undergoes only *small-amplitude* excursions from $y^\ddagger = 0$.[5]

It is this assumption which leads to the constraint $y = y^\ddagger$. The small-amplitude excursion assumption is restrictive and we hope to lift it in the future. However, Wilson and co-workers have shown for their model S_N2 systems[8] (see Sec. IV) that the early-time excursions of the asymmetric stretch coordinate are, indeed, small.

One disadvantage of the familiar[15,18] phenomenological equations of motion for reaction coordinate dynamics is that it is difficult to connect these one-dimensional descriptions with the actual multidimensional barrier crossing dynamics. In contrast, Eq. (2.6) is a molecularly based equation of motion and, therefore, may be connected to the underlying multidimensional processes.

Thus it is of interest to examine the physical interpretations of the generalized force terms appearing in Eq. (2.6). We will see that these generalized forces may be connected to

the actual forces experienced by the solute when moving on a multidimensional potential surface. Moreover, we will see that these physical interpretations are considerably more subtle than one might expect given the simplicity of the phenomenological descriptions.

We will focus, in particular, on $F_{\mathrm{MIP}}[y]$, the generalized force associated with $W_{\mathrm{MIP}}[y]$ (see Fig. 2). Given our earlier discussion of $W_{\mathrm{MIP}}[y]$ (see the Introduction), it is evident that $F_{\mathrm{MIP}}[y]$ is associated with the "rigid-cage" or frozen-solvent limit of reaction dynamics. $F_{\mathrm{MIP}}[y]$, in fact, determines the equilibrium rate constant in that limit.

To visualize the physical interpretation of $F_{\mathrm{MIP}}[y]$, first consider the ensemble of solute geometries for which $y = y^{\ddagger} = 0$. We will refer to this as the transition-state (TS) ensemble. For triatomic $A + BC$ systems, for example, the TS ensemble consists of the liquid-phase TS geometry of the solute and all geometries which may be obtained from it by symmetric stretch and bend deformations keeping the asymmetric stretch coordinate fixed. Such deformations move the solute along its liquid-phase potential-energy surface in directions orthogonal to the reaction path with y maintained at $y^{\ddagger}$.

Assume that the solute is initially fixed in the liquid at some arbitrary[28] value z_e of its translational–rotational coordinates and at one of its TS ensemble geometries $y^{\ddagger} z_i$, where z_i are the solute vibrational coordinates. The initial solute configuration is therefore $y^{\ddagger} z$, where $z = z_i z_e$.

Next, assume that the solute undergoes a reactive attempt. We define such an attempt as an excursion which removes the solute from its initial TS ensemble geometry $y^{\ddagger} z_i$ and places it in a new non-TS ensemble geometry. [The basis of this definition of a reactive attempt is that the equilibrium rate constant may be computed (see Sec. II A) as a canonical ensemble average over all solution trajectories which initiate with the solute in a TS ensemble geometry.]

Assume a reactive attempt in which y changes from $y^{\ddagger}$ to y while the remaining degrees of freedom of the solution remain fixed[29] at their initial values zq. The total generalized force after this reactive displacement will be denoted by $F[y;zq]$. Next, average $F[y;zq]$ first over the canonical distribution of solvent configurations q for a fixed solute configuration $y^{\ddagger} z$ and second over the canonical distribution of TS ensemble geometries $y^{\ddagger} z_i$. The result of this double-averaging process is independent of the coordinates z_e (Ref. 28) and is, in fact, equal to $F_{\mathrm{MIP}}[y]$.

The physical interpretation of $F_{\mathrm{MIP}}[y]$ is now evident. It is the ensemble-averaged generalized force exerted on the reaction coordinate after a displacement $y^{\ddagger} \to y$ assuming the time required for the displacement is infinitely short. The remaining terms in Eqs. (2.6) correct $F_{\mathrm{MIP}}[y]$ for the ensemble-averaged effects of relaxation of the zq degrees of freedom arising from the finite time of the displacement, the integral kernel term, and for spatial-temporal fluctuations which would occur in the absence of the displacement, the fluctuating force $\tilde{F}_{0(t)}(t)$.

C. Some simplifying approximations

To keep the analysis presented in the remainder of the paper free from encumbering detail, we next introduce two approximations which are additional to those inherent in the partial-clamping model. These additional approximations, which we hope to remove in more refined future treatments, are as follows.

(i) We neglect fluctuations of the restoring force $[\partial F_0/\partial y^{\ddagger}]y$ from its ensemble-averaged value $\langle \partial F/\partial y \rangle_0 y$. From the standpoint of the analysis of Sec. III, this approximation amounts to suppressing fluctuations in the frequency ω_e of the cage potential $W_c[y,\tilde{F}]$ [see Eq. (3.31a)] while retaining fluctuations in the position of its minimum.

(ii) We assume that the reaction coordinate y is separable in the gas phase. This separability approximation amounts to neglecting kinetic- and potential-energy couplings, discussed by Marcus,[30] Miller, Handy, and Adams,[31] and others which contribute to the gas-phase part of $F_{\mathrm{MIP}}[y]$.

Given assumption (i), the fluctuating force $\tilde{F}_{0(t)}(t)$ defined in Eq. (2.6b) reduces to

$$\tilde{F}_{0(t)}(t) \doteq \tilde{F}_0(t) \equiv F_0(t) - \langle F \rangle_0 . \tag{2.8}$$

Assumption (ii) implies that the gas-phase contribution $F_g[y]$ to $F_{\mathrm{MIP}}[y]$ may be written as

$$F_g[y] = -\frac{dV_g[y]}{dy} . \tag{2.9}$$

The potential energy $V_g[y]$ appearing in Eq. (2.9) is the gas-phase potential-energy surface of the solute evaluated for the solute MERP geometry associated with the reaction coordinate value y. However, recall (Sec. II A) that the one-to-one association between reaction coordinate values and solute geometries must be made for the *liquid-phase* potential-energy surface of the solute. Thus to rigorously evaluate $V_g[y]$, one must deal with the difficult problem of determining the liquid-phase reaction path. In this initial study of activated barrier crossing in liquids, we will bypass this problem by approximating $V_g[y]$ by the MERP potential of the gas-phase potential-energy surface. We believe that this approximation will not lead to erroneous qualitative conclusions. Moreover, the approximation will enable us to use the gas-phase MERP potential for the $Cl^- + CH_3Cl$ reaction computed by Chandrasekhar and co-workers[17] in applications of the theory developed in Sec. III (see, e.g., Fig. 2).

Using Eqs. (2.8) and (2.9), the equation of motion (2.6) becomes

$$\ddot{y}(t) = -\frac{dV_g[y(t)]}{dy(t)} + \langle F \rangle_0 + \left\langle \frac{\partial F}{\partial y} \right\rangle_0 y(t) + \beta \int_0^t \langle \tilde{F}(t-\tau)\tilde{F} \rangle_0 y(\tau) d\tau + \tilde{F}_0(t), \tag{2.10a}$$

where

$$\tilde{F}_0(t) = F_0(t) - \langle F \rangle_0 . \tag{2.10b}$$

III. EARLY-TIME DYNAMICS, STATIC FLUCTUATIONS, AND THE INSTANTANEOUS POTENTIAL

A. Early-time dynamics

The importance of the rigid-cage or frozen-solvent limit of the actual solvent dynamics in determining the solute motions in the earliest stages ($\sim$10–20 fs) of a reactive attempt

has been demonstrated by Wilson and co-workers[8] for their model S_N2 systems. These workers have, moreover, established that the transmission coefficient κ for these systems is largely determined by barrier recrossing processes occurring in the same early-time regime. Thus both the magnitude and variation of the transmission coefficient (see Sec. V) and the early-time solute dynamics are importantly influenced by rigid-cage behavior. Moreover, given the discussion in the Introduction, it appears likely that such behavior will importantly influence reaction attributes in many other liquid-phase systems.

We, therefore, present an analysis of the short-time-scale rigid-cage limit based on the equation of motion (2.10). This analysis and, in particular, our treatment of cage fluctuations is motivated, in part, by the discussion due to Bergsma *et al.*[8(a)] summarized in the Introduction. We begin by combining Eqs. (2.10a) and (2.10b) and evaluating all liquid-state generalized forces in the $t = 0$ limit. This yields the following short-time-scale equation of motion for the reaction coordinate

$$\ddot{y}(t) = F_{\rm IP}[y(t),\tilde{F}], \tag{3.1}$$

where $F_{\rm IP}[y,\tilde{F}]$ is the generalized force acting on the reaction coordinate after a displacement $y^\ddagger \to y$ conditional that the zq coordinates remain fixed[29] at their initial values during the displacement. We will refer to $F_{\rm IP}[y,\tilde{F}]$ as the *instantaneous force*. The explicit form of $F_{\rm IP}[y,\tilde{F}]$ is

$$F_{\rm IP}[y,\tilde{F}] = -\frac{dV_g[y]}{dy} + \tilde{F} + \langle F\rangle_0 + \left\langle\frac{\partial F}{\partial y}\right\rangle_0 y, \tag{3.2}$$

where $\tilde{F} = \tilde{F}[y^\ddagger zq] \equiv \tilde{F}_0[t=0]$ is the initial value of the fluctuating force $\tilde{F}_0(t)$ defined in Eq. (2.10b). ($\tilde{F} + \langle F\rangle_0$ is analogous to the "solvent bias force" of Bergsma *et al.*[8(a)] discussed in the Introduction.)

Next, note that the generalized force $F_{\rm MIP}[y]$, discussed in Sec. II B, is the ensemble average of $F_{\rm IP}[y,\tilde{F}]$; i.e.,

$$F_{\rm MIP}[y] = \langle F_{\rm IP}[y,\tilde{F}]\rangle_0 = F_g[y] + \langle F\rangle_0 + \left\langle\frac{\partial F}{\partial y}\right\rangle_0 y. \tag{3.3}$$

To obtain Eq (3.3) from Eq. (3.2) we have used Eq. (2.7) and (2.9) and the fact that $\langle\tilde{F}\rangle_0 = 0$.

B. The instantaneous potential

From Eq. (3.2) it is evident that $F_{\rm IP}[y,\tilde{F}]$ is a conservative force. Thus a potential-energy function $W_{\rm IP}[y,\tilde{F}]$ is associated with $F_{\rm IP}[y,\tilde{F}]$; i.e.,

$$F_{\rm IP}[y,\tilde{F}] = -\frac{\partial W_{\rm IP}[y,\tilde{F}]}{\partial y}. \tag{3.4}$$

We will refer to $W_{\rm IP}[y,\tilde{F}]$ as the *instantaneous potential*. Comparison of Eqs. (3.2) and (3.4) yields the following form for $W_{\rm IP}[y,\tilde{F}]$:

$$W_{\rm IP}[y,\tilde{F}] = V_g[y] - [\tilde{F} + \langle\tilde{F}\rangle_0]y - \frac{1}{2}\left\langle\frac{\partial F}{\partial y}\right\rangle_0 y^2 + W[\tilde{F}], \tag{3.5}$$

where $W[\tilde{F}]$ is an integration constant and is, hence, independent of y. (Strictly speaking $W[\tilde{F}]$ is a function of $y^\ddagger zq$ rather than of $\tilde{F} = \tilde{F}[y^\ddagger zq]$. However, within the stochastic model developed below the integration constant depends only on $\tilde{F}$. Hence the designation $W[\tilde{F}]$.)

C. Stochastic model for $W_{\rm IP}[y,\tilde{F}]$: The Gaussian noise approximation

The instantaneous potential $W_{\rm IP}[y,\tilde{F}]$ is of interest since, with a suitable choice of the integration constant $W[\tilde{F}]$, it is closely related to the actual early-time potential energy of the liquid solution. Thus in this section and in Sec. III F we develop a stochastic model for $W_{\rm IP}[y,\tilde{F}]$. This model will permit explicit calculation of $W_{\rm IP}[y,\tilde{F}]$ for specific solute–solvent systems. Examples of such calculations will be given elsewhere.

We begin with the assumption that the fluctuating force $\tilde{F}_0(t)$ [Eq. (2.10b)] may be modeled by Gaussian noise.[15(a)] [The Gaussian noise assumption is also made in the derivation (Appendix B) of the transmission coefficient formula, Eqs. (1.1) and (1.2). Thus the treatment of static fluctuations developed in this section is consistent with the rate-constant models described in the Introduction.] Given the Gaussian noise assumption for $\tilde{F}_0(t)$ it follows that $\tilde{F} = \tilde{F}_0[t=0]$ is a Gaussian random variable with zero mean (since $\langle\tilde{F}\rangle_0 = 0$). The probability distribution function (PDF) for $\tilde{F}$ is, therefore

$$P[\tilde{F}] = (2\pi\langle\tilde{F}^2\rangle_0)^{-1/2}\exp\left(-\frac{1}{2}\frac{\tilde{F}^2}{\langle\tilde{F}^2\rangle_0}\right). \tag{3.6}$$

Notice, within the stochastic model of Eq. (3.6), the instantaneous potential is determined probabilistically since it depends [Eq. (3.5)] on the random variable $\tilde{F}$. The probability of a particular instantaneous potential $W_{\rm IP}[y,\tilde{F}]$ is equal to the probability of the corresponding fluctuating force $\tilde{F}$ and hence is proportional to the PDF $P[\tilde{F}]$.

D. The most probable instantaneous potential

The potential $W_{\rm MIP}[y]$, discussed in the Introduction, may be obtained by setting $\tilde{F} = 0$ in Eq. (3.5) to yield

$$W_{\rm MIP}[y] \equiv W_{\rm IP}[y,\tilde{F}=0] = V_g[y] + W[\tilde{F}=0] - \langle F\rangle_0 y - \frac{1}{2}\left\langle\frac{\partial F}{\partial y}\right\rangle_0 y^2. \tag{3.7}$$

Within the stochastic model of Eq. (3.6), however, $\tilde{F} = 0$ is the most probable fluctuating force. For this reason, we will refer to $W_{\rm MIP}[y]$ as the *most probable instantaneous potential*. [This designation, however, is only strictly correct within the stochastic model of Eq. (3.6).]

Next, we show that $W_{\rm MIP}[y]$ is the potential which governs *ensemble-averaged* early-time reaction coordinate dynamics in the liquid. We first note that $W_{\rm MIP}[y]$ is the potential associated with $F_{\rm MIP}[y]$; i.e.,

$$F_{\rm MIP}[y] = -\frac{dW_{\rm MIP}[y]}{dy}. \tag{3.8}$$

Equation (3.8) follows from Eqs. (2.9), (3.3), and (3.7). Comparison of Eqs. (3.3) and (3.8) then shows that

$W_{\mathrm{MIP}}[y]$ determines the early-time ensemble-averaged force.

E. $W_{\mathrm{MIP}}[y]$ versus $W_{\mathrm{PMF}}[y]$

The potential of mean force $W_{\mathrm{PMF}}[y]$ provides the conventional[14] basis for interpreting liquid-phase activated barrier crossing phenomena. Given the discussion in the Introduction, however, it is evident that the most probable instantaneous potential $W_{\mathrm{MIP}}[y]$ provides a more satisfactory framework for describing the liquid-phase barrier crossing processes which occur in typical chemical reactions. Thus it is of interest to compare and contrast $W_{\mathrm{MIP}}[y]$, the short-time-scale potential, and $W_{\mathrm{PMF}}[y]$, the adiabatic potential.

We begin with the following decomposition of $W_{\mathrm{PMF}}[y]$:

$$W_{\mathrm{PMF}}[y] = V_g[y] + w^{(2)}[y], \tag{3.9}$$

where $V_g[y]$ and $w^{(2)}[y]$ are, respectively, the gas-phase and liquid-phase contributions to $W_{\mathrm{PMF}}[y]$. Note that $w^{(2)}[y]$ is the cavity potential of the reaction coordinate. The generalized force $\langle F\rangle_0$ is determined in terms of the cavity potential via

$$\langle F\rangle_0 = -\frac{\partial w^{(2)}[y]}{\partial y}. \tag{3.10}$$

Next expand Eq. (3.9) to quadratic order in y about $y = y^\ddagger = 0$. This expansion yields the following parabolic approximation to $W_{\mathrm{PMF}}[y]$:

$$W_{\mathrm{PMF}}[y] \doteq W_{\mathrm{PMF}}[y^\ddagger] - (F_g[y^\ddagger] + \langle F\rangle_0)y - \frac{1}{2}\left(\frac{\partial F_g[y^\ddagger]}{\partial y^\ddagger} + \frac{\partial \langle F\rangle_0}{\partial y^\ddagger}\right)y^2, \tag{3.11}$$

where we have used Eqs. (2.9), (3.9), and (3.10) to obtain Eq. (3.11). We will further use the fact that $W_{\mathrm{PMF}}[y^\ddagger]$ is approximately equal to the liquid-phase activation energy E_A of the solute; i.e.,

$$E_A \doteq W_{\mathrm{PMF}}[y^\ddagger] = w^{(2)}[y^\ddagger] + V_g[y^\ddagger]. \tag{3.12}$$

Next, recall (Sec. II A) that the liquid-phase TS of the solute coincides with the saddle point of its potential of mean force surface. A consequence is that the total ensemble-averaged force $F_T[y^\ddagger]$ acting on the reaction coordinates vanishes at the TS; i.e.,

$$F_T[y^\ddagger] \equiv F_g[y^\ddagger] + \langle F\rangle_0 = 0. \tag{3.13}$$

Using Eqs. (3.12) and (3.13), Eq. (3.11) simplifies to

$$W_{\mathrm{PMF}}[y] \doteq E_A - \frac{1}{2}\left(\frac{\partial F_g[y^\ddagger]}{\partial y^\ddagger} + \frac{\partial \langle F\rangle_0}{\partial y^\ddagger}\right)y^2. \tag{3.14}$$

We next perform a similar parabolic analysis of $W_{\mathrm{MIP}}[y]$ defined in Eq. (3.7). We begin with the following choice of the integration constant $W[\tilde{F}=0]$:

$$W[\tilde{F}=0] = w^{(2)}[y^\ddagger]. \tag{3.15}$$

With use of Eq. (3.15), a parabolic expansion of Eq. (3.7) yields

$$W_{\mathrm{MIP}}[y] \doteq E_A - \frac{1}{2}\left(\frac{\partial F_g[y^\ddagger]}{\partial y^\ddagger} + \left\langle\frac{\partial F}{\partial y}\right\rangle_0\right)y^2. \tag{3.16}$$

$W_{\mathrm{MIP}}[y]$ and $W_{\mathrm{PMF}}[y]$ may now be contrasted. Comparison of Eqs. (3.14) and (3.16) shows the following.

(i) The two potentials coincide at the TS, $y = y^\ddagger$, where they are equal to the liquid-phase activation energy E_A.

(ii) Both potentials have their maxima at the TS. ($W_{\mathrm{MIP}}[y]$ may actually have its minimum at the TS; see Sec. III K).

(iii) Thus the two potentials coincide in the immediate neighborhood of the TS. They, however, differ once their quadratic order terms become non-negligible since $\partial\langle F\rangle_0/\partial y^\ddagger \neq \langle \partial F/\partial y\rangle_0$. *This difference* (see the Introduction) *is central to the physically correct description of reaction dynamics in liquids.*

We conclude this comparison of $W_{\mathrm{MIP}}[y]$ and $W_{\mathrm{PMF}}[y]$ by briefly describing the distinction between the quantities $\langle \partial F/\partial y\rangle_0$ and $\partial\langle F\rangle_0/\partial y^\ddagger$. A more complete discussion is given elsewhere.[1(a)] We begin by defining the frequencies ω_e and Ω_0 by

$$\omega_e^2 = -\left\langle\frac{\partial F}{\partial y}\right\rangle_0 \tag{3.17a}$$

and

$$\Omega_0^2 = -\frac{\partial\langle F\rangle_0}{\partial y^\ddagger}. \tag{3.17b}$$

The frequency ω_e determines the ensemble-averaged liquid-phase force, $\omega_e^2 y$, which acts on the reaction coordinate *immediately after* a small instantaneous displacement $y^\ddagger \to y$. The displacement removes the system from thermodynamic equilibrium. Therefore the force $-\omega_e^2 y$ works to reestablish equilibrium by restoring the reaction coordinate to its initial value $y^\ddagger = 0$. This restoring property of the force $-\omega_e^2 y$ is responsible for the fact that $W_{\mathrm{MIP}}[y]$ is a *bound* potential (see Fig. 2).

The frequency Ω_0 determines the ensemble-averaged liquid-phase force $-\Omega_0^2 y$ exerted on the reaction coordinate after the zq degrees of freedom have had time to *fully relax* in response to the displacement. Relaxation returns the system to thermodynamic equilibrium and thus decreases the magnitude of the initial nonequilibrium restoring force. Because of this relaxation, $W_{\mathrm{PMF}}[y]$, unlike $W_{\mathrm{MIP}}[y]$, can be an *unbound* potential (see Fig. 1). An additional consequence of the relaxation is the inequality

$$\omega_e^2 > \Omega_0^2. \tag{3.18}$$

F. Stochastic model for $W_{\mathrm{IP}}[y,\tilde{F}]$: Choice of the integration constant

Comparison of Eqs. (3.5), (3.12), (3.15), and (3.17a) yields the following form for the instantaneous potential $W_{\mathrm{IP}}[y,\tilde{F}]$:

$$W_{\mathrm{IP}}[y,\tilde{F}] = E_A + V_g[y] - V_g[y^\ddagger] + \tfrac{1}{2}\omega_e^2 y^2 - [\tilde{F} + \langle F\rangle_0]y + W[\tilde{F}] - W[\tilde{F}=0], \tag{3.19}$$

where, recall, $W[\tilde{F}] - W[\tilde{F}=0]$ is an integration constant.

We next discuss the choice of this integration constant. To motivate this choice we first consider $W_{\mathrm{MIP}}[y] = W_{\mathrm{IP}}[y,\tilde{F}=0]$ defined in Eq. (3.7). Setting $\tilde{F}=0$ in Eq. (3.19) yields the following form for $W_{\mathrm{MIP}}[y]$:

$$W_{\mathrm{MIP}}[y] = E_A + (V_g[y] - V_g[y^\ddagger] + \tfrac{1}{2}\omega_e^2 y^2 - \langle F\rangle_0 y). \tag{3.20}$$

The terms in Eq. (3.20) have the following interpretations. The liquid-phase activation energy E_A is the ensemble-averaged work required to assemble the liquid solution conditional that the reaction coordinate is fixed at $y=y^\ddagger$. (We take the free energy of the pure liquid as the zero of energy.) The term in parentheses is the additional ensemble-averaged work required for a small instantaneous displacement of the reaction coordinate from $y^\ddagger$ to y.

It would be desirable to choose the integration constant so that $W_{\mathrm{IP}}[y,F]$ is a sum of work terms analogous to those just discussed for $W_{\mathrm{MIP}}[y]$. These terms, however, should be works with the solution coordinates other than y fixed at zq rather then ensemble-averaged works.

This may be accomplished by choosing $W[\tilde{F}]$ to be equal to the liquid-phase work required to assemble the solution at configuration zq conditional that y is fixed at $y^\ddagger$. We will denote this liquid-phase work by $w^{(2)}[y^\ddagger zq]$. With this choice of $W[\tilde{F}]$, the integration constant $W[\tilde{F}] - W[\tilde{F}=0]$ has a simple interpretation. Given Eq. (3.15), it is the work $w[\tilde{f}] \equiv w^{(2)}[y^\ddagger zq] - w^{(2)}[y^\ddagger]$ required to create the fluctuation $\tilde{f}$ from equilibrium which places the system in the configuration $y^\ddagger zq$. Moreover, if this choice of $W[\tilde{F}]$ is made, $W_{\mathrm{IP}}[y,\tilde{F}]$ may be interpreted as follows. It is the work required to first activate the solute given that the system is in thermodynamic equilibrium, to next create the fluctuation $\tilde{f}$ from equilibrium, and to lastly instantaneously displace the reaction coordinate from $y^\ddagger$ to y in the presence of the fluctuation. That is, $W_{\mathrm{MIP}}[y]$ and $W_{\mathrm{IP}}[y,\tilde{F}]$ would have parallel interpretations as the works required for activation (i.e., placing the reaction coordinate at $y^\ddagger$) followed by an instantaneous displacement $y^\ddagger \to y$; $W_{\mathrm{MIP}}[y]$ for the ensemble-averaged case and $W_{\mathrm{IP}}[y,\tilde{F}]$ for the case that the activated configuration of the liquid solution is $y^\ddagger zq$.

Unfortunately, it is difficult to obtain a convenient result for the liquid-phase work $w^{(2)}[y^\ddagger zq]$, and as a result we must make a different choice of the integration constant $W[\tilde{F}]$. We next introduce a stochastic model for $W[\tilde{F}]$ which captures, in a qualitative manner, the main features of the physics just discussed.

We begin by noting that the probability $p[\tilde{f}]$ of the fluctuation $\tilde{f}$ is proportional to the Boltzmann factor $\exp(-\beta w^{(2)}[y^\ddagger zq])$. Equivalently $\ln p[\tilde{f}] \propto -\beta w^{(2)}[y^\ddagger zq]$ or, with the choice of integration constant discussed above, $\ln p[\tilde{f}] \propto -\beta W[\tilde{F}]$. Also, note that if a fluctuation $\tilde{f}$ is present, the fluctuating force is nonvanishing and has the value $\tilde{F}=\tilde{F}[y^\ddagger zq]$. The stochastic model is based on the assumption that the probability of the fluctuation $\tilde{f}$, $p[\tilde{f}]$, is proportional to the probability $P[\tilde{F}]$ of the corresponding fluctuating force $\tilde{F}$.[32] This assumption is equivalent to the following choice of the integration constant:

$$-\beta(W[\tilde{F}] - W[\tilde{F}=0]) = \ln\left(\frac{P[\tilde{F}]}{P[\tilde{F}=0]}\right) = -\frac{1}{2}\frac{\tilde{F}^2}{\langle\tilde{F}^2\rangle_0}, \tag{3.21}$$

where the final form of Eq. (3.21) follows from Eq. (3.6). Comparison of Eqs. (3.19) and (3.21) then yields the following stochastic model for $W_{\mathrm{IP}}[y,\tilde{F}]$:

$$W_{\mathrm{IP}}[y,\tilde{F}] = E_A + V_g[y] - V_g[y^\ddagger] + \frac{1}{2}\omega_e^2 y^2 - [\tilde{F} + \langle F\rangle_0]y + \frac{1}{2}\frac{k_B T}{\langle\tilde{F}^2\rangle_0}\tilde{F}^2. \tag{3.22}$$

G. The cage potential

We next introduce the *cage potential* $W_c[y,\tilde{F}]$ via the definition

$$W_c[y,\tilde{F}] = \frac{1}{2}\omega_e^2 y^2 - [\tilde{F} + \langle F\rangle_0]y + \frac{1}{2}\frac{k_B T}{\langle\tilde{F}^2\rangle_0}\tilde{F}^2. \tag{3.23}$$

Comparison of Eqs. (3.22) and (3.23) shows that $W_{\mathrm{IP}}[y,\tilde{F}]$ may be rewritten in terms of $W_c[y,\tilde{F}]$ in the following manner:

$$W_{\mathrm{IP}}[y,\tilde{F}] = E_A + V_g[y] - V_g[y^\ddagger] + W_c[y,\tilde{F}]. \tag{3.24}$$

We define the most probable cage potential $W_c[y]$ by $W_c[y] = W_c[y,\tilde{F}=0]$. Given this definition relationships analogous to Eqs. (3.23) and (3.24) hold, namely,

$$W_c[y] = \tfrac{1}{2}\omega_e^2 y^2 - \langle F\rangle_0 y \tag{3.25}$$

and

$$W_{\mathrm{MIP}}[y] = E_A + V_g[y] - V_g[y^\ddagger] + W_c[y]. \tag{3.26}$$

Loosely speaking the cage potentials govern the instantaneous liquid-phase restoring forces acting on the reaction coordinate and as a result are central to the liquid-phase effect on reaction dynamics. More precise physical interpretations will be developed in Sec. III I.

In order to more clearly reveal the effects of the cage potentials on reaction coordinate motion we next recast them into an alternative form, Eqs. (3.31). We begin by defining the friction kernel of the reaction coordinate $\beta(t)$ by

$$\beta(t) = (k_B T)^{-1}\langle\tilde{F}(t)\tilde{F}\rangle_0. \tag{3.27}$$

Following an argument presented elsewhere,[1(a)] one may show $\beta(t=0) = \omega_e^2 - \Omega_0^2$, where ω_e^2 and Ω_0^2 are defined in Eq. (3.17). It then follows from Eq. (3.27) that

$$\langle\tilde{F}^2\rangle_0 = k_B T(\omega_e^2 - \Omega_0^2) > 0, \tag{3.28}$$

where the inequality holds because $\langle\tilde{F}^2\rangle_0 > 0$. (Notice that Eq. (3.28) constitutes a proof of the inequality $\omega_e^2 > \Omega_0^2$ [Eq. (3.18)] developed earlier via a physical argument.)

Next, we note that since $W_c[y,\tilde{F}]$ is a quadratic form in y and $\tilde{F}$, it has an exact quadratic expansion about its extremum $y^*,\tilde{F}^*$. This extremum is determined by the conditions

$$\frac{\partial W_c[y^*,\tilde{F}^*]}{\partial y^*}=\frac{\partial W_c[y^*,\tilde{F}^*]}{\partial F^*}=0.$$

With use of Eq. (3.23) and (3.28), it follows that the quadratic expansion takes the following form:

$$W_c[y,\tilde{F}]-W_c[y^*,\tilde{F}^*]$$
$$=\frac{1}{2}\omega_e^2[y-y^*]^2-[y-y^*][\tilde{F}-\tilde{F}^*]$$
$$+\frac{1}{2}\frac{[\tilde{F}-\tilde{F}^*]^2}{\omega_e^2-\Omega_0^2}, \tag{3.29}$$

where the coordinates of the extremum are given by

$$y^*=\Omega_0^{-2}\langle F\rangle_0 \tag{3.30a}$$

and

$$\tilde{F}^*=\Omega_0^{-2}[\omega_e^2-\Omega_0^2]\langle F\rangle_0. \tag{3.30b}$$

Equation (3.29) may recast to yield

$$W_c[y,\tilde{F}]-W_c[y^*,\tilde{F}^*]$$
$$=\frac{1}{2}\omega_e^2[(y-y^*)-\omega_e^{-2}(\tilde{F}-\tilde{F}^*)]^2$$
$$+\frac{1}{2}\frac{\Omega_0^2}{\omega_e^2}\frac{[\tilde{F}-\tilde{F}^*]^2}{\omega_e^2-\Omega_0^2}\geqslant 0, \tag{3.31a}$$

where the inequality in Eq. (3.31a) holds since $\omega_e^2>\Omega_0^2$.

Equation (3.31a) shows that $W_c[y,\tilde{F}]-W_c[y^*,\tilde{F}^*]$ is a positive definite quadratic form.[33] Thus $W_c[y,\tilde{F}]$ is mathematically identical to the potential energy of a mechanically stable pair of coupled harmonic oscillators with coordinates y and $\tilde{F}$. The position of mechanical equilibrium of this oscillator system is the extremum point $y^*,\tilde{F}^*$. (Note that our modeling of solvent fluctuations by the fluctuations of a harmonic oscillator $\tilde{F}$ is in the spirit of the Marcus[34] electron transfer theory.)

Finally, it follows from Eq. (3.31a) that $W_c[y]=W_c[y,\tilde{F}=0]$ [Eq. 3.25)] may be recast as

$$W_c[y]=W_c[y^*,\tilde{F}^*]+\frac{1}{2}\omega_e^2[y-(y^*-\omega_e^{-2}\tilde{F}^*)]^2$$
$$+\frac{1}{2}\frac{\Omega_0^2}{\omega_e^2}\frac{(\tilde{F}^*)^2}{\omega_e^2-\Omega_0^2}. \tag{3.31b}$$

H. Symmetric reactions

The applications presented in later sections are performed for the special case of *symmetric* $A+BC$ reactions. We, therefore, next specialize our expressions for the cage potential to this special case. For symmetric reactions $W_c[-y]=W_c[y]$. It therefore follows from Eq. (3.31b) that $y^*-\omega_e^{-2}F^*=0$. Further comparison with Eqs. (3.30) then yields

$$y^*=\tilde{F}^*=\langle F\rangle_0=0 \quad \text{(symmetric reactions)}. \tag{3.32}$$

Comparison of Eqs. (3.31) and (3.32) yields the following form for the cage potentials for symmetric reactions:

$$W_c[y,\tilde{F}]=\frac{1}{2}\omega_e^2[y-\omega_e^{-2}\tilde{F}]^2+\frac{1}{2}\frac{\Omega_0^2}{\omega_e^2}\frac{\tilde{F}^2}{\omega_e^2-\Omega_0^2} \tag{3.33a}$$

and

$$W_c[y]=\tfrac{1}{2}\omega_e^2y^2 \quad \text{(symmetric reactions)}. \tag{3.33b}$$

I. Interpretation of the cage potentials

Next, we briefly discuss the physical interpretations of the cage potentials. These interpretations are simplest for the case of symmetric reactions and, therefore, we will restrict ourselves, in this section, to that special case.

The precise physical interpretation of $W_c[y]$ [Eq. (3.33b)] follows from the interpretation of $F_{\text{MIP}}[y]$ given in Sec. II B. Briefly stated, $W_c[y]$ is the liquid-phase contribution to the ensemble-averaged work required for the instantaneous displacement $y^\ddagger\to y$. This work is a positive monotonically increasing function of $y-y^\ddagger=y$. Thus a displacement of the reaction coordinate away from its TS value $y^\ddagger$ is resisted by $W_c[y]$. Hence $W_c[y]$ works to restore the reaction coordinate back to its TS value $y^\ddagger=0$ (see Fig. 2).

The cage potential $W_c[y,\tilde{F}]$ corrects $W_c[y]$ for the effects of deviations from the ensemble-averaged description. These deviations give rise to a nonvanishing fluctuating force $\tilde{F}$ which produces a work $-\tilde{F}y$ [see Eq. (3.23)] which is additional to the ensemble-averaged work $W_c[y]$. For $\tilde{F}<0$, the work is positive for a displacement into the product valley ($y>0$) and, hence, *resists* a reactive attempt $y^\ddagger\to y>0$. Conversely, for $\tilde{F}>0$ the extra work *promotes* such a reactive attempt.

This may be seen in an alternative manner from the result for $W_c[y,\tilde{F}]$ given in Eq. (3.33a). This result shows that, for fixed $\tilde{F}$, $W_c[y,\tilde{F}]$ has its minimum at $y_{\min}=\omega_e^{-2}\tilde{F}$ and, moreover, is a positive monotonically increasing function of $y-y_{\min}$. Thus $W_c[y,\tilde{F}]$ works to restore the reaction coordinate to $y_{\min}$. However $y_{\min}$ occurs in the product valley for $\tilde{F}>0$ and in the reactant valley for $\tilde{F}<0$. Thus the cage potential promotes the reaction if $\tilde{F}>0$ and resists the reaction if $\tilde{F}<0$.

These considerations have obvious implications for the early-time barrier recrossing processes discussed in Sec. III A. Namely, barrier recrossing processes of the type $y^\ddagger\to y>0\to y^\ddagger\to y<0$ are promoted by fluctuations if $\tilde{F}<0$ and are resisted by fluctuations if $\tilde{F}>0$.

Wilson and co-workers[8] have discussed such early-time barrier recrossing processes in the context of their MD simulations of model symmetric S_N2 reactions. They find that "reactant-like" static solvent density fluctuations promote barrier recrossing processes of the type just discussed while "product-like" static solvent density fluctuations impede such barrier recrossing processes. In fact, for their model systems barrier recrossing from products to reactants nearly always occurred *only* in the presence of reactant-like static solvent density fluctuations.

Given this discussion, it is tempting to identify fluctuating forces for which $\tilde{F}>0$ ($W_c[y,\tilde{F}]$ has its minimum in the product valley) with product-like solvent density fluctuations and fluctuating forces for which $\tilde{F}<0$ ($W_c[y,\tilde{F}]$ has its minimum in the reactant valley) with reactant-like solvent density fluctuations. Such an identification is not, how-

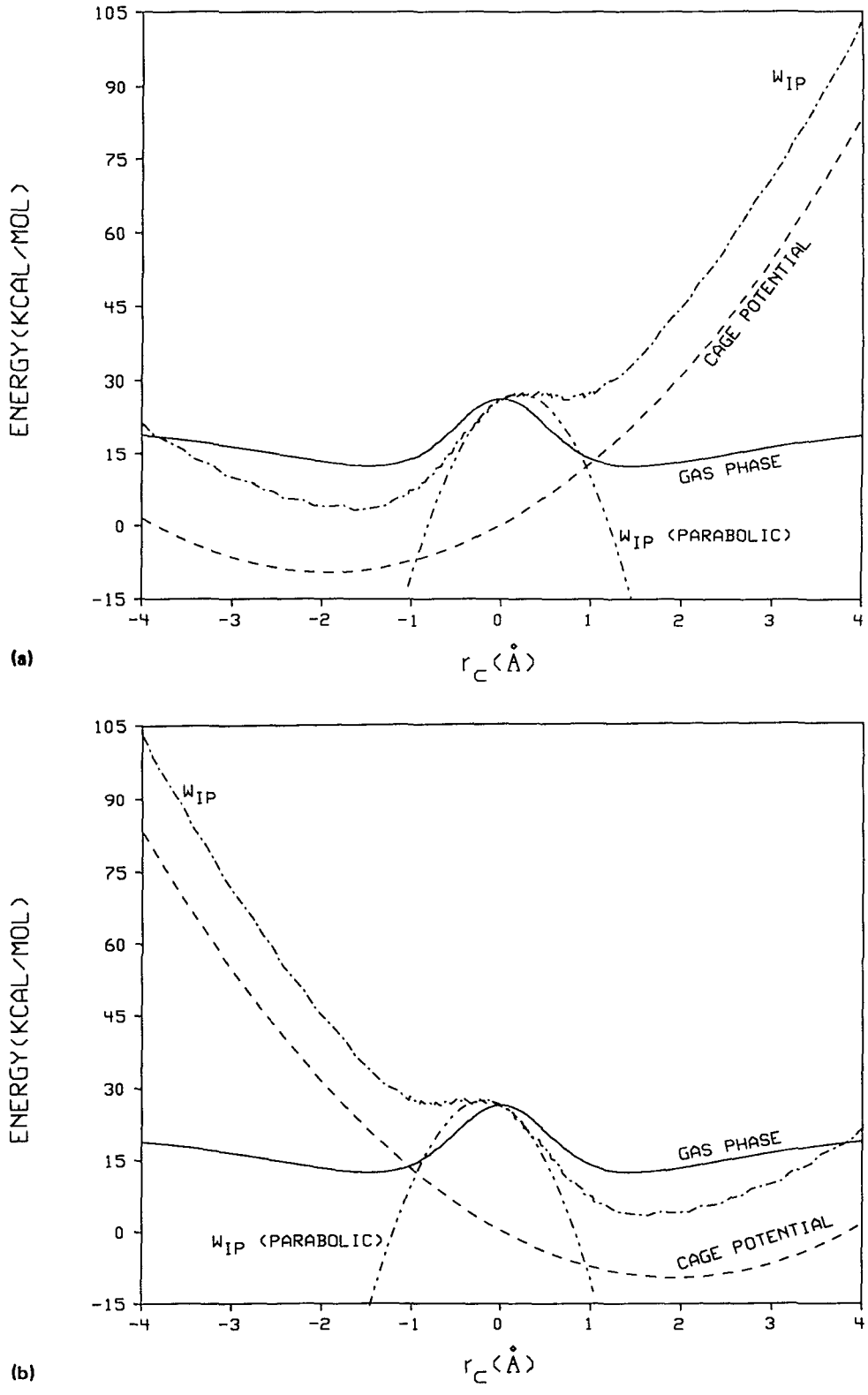

FIG. 3. Reaction-path potentials for the aqueous $Cl^- + CH_3Cl$ S_N2 system near standard conditions. (a) Same as Fig. 2 except for a representative "reactant-like" fluctuation [fluctuating force $\tilde{F} = -(\langle \tilde{F}^2 \rangle_0)^{1/2}$]. Notice that the barrier in the product valley inhibits excursions from the TS of $\gtrsim +0.03$ Å for the reaction coordinate energies $\lesssim 550$ K. (b) Same as Fig. 2 except for a representative "product-like" fluctuation.

ever, strictly correct since the fluctuating force $\tilde{F}$ depends on the solute z coordinates as well as the solvent q coordinates and since, in general, a one-to-one correspondence between forces $\tilde{F}$ and zq values does not exist.

For convenience, we will henceforth refer to $\tilde{F}>0$ as a product-like fluctuation and $\tilde{F}<0$ as a reactant-like fluctuation. The qualitative nature of this terminology must, however, be kept in mind.

The points just made are illustrated in Fig. 3, where we plot $W_{IP}[y,\tilde{F}]$ for the aqueous $Cl^- + CH_3Cl$ system for representative [see Eq. (3.6)] reactant-like and product-like fluctuations, $\tilde{F} = \pm(\langle \tilde{F}^2 \rangle_0)^{1/2}$. These plots and also

Fig. 2 are constructed by a procedure given in Sec. IV C. (As discussed in Sec. IV C, Figs. 2 and 3 have only qualitative significance.) Notice that for the reactant-like fluctuation [Fig. 3(a)], $W_{IP}[y,\tilde{F}]$ has an approximately 550 K barrier in the product valley which induces recrossings into the reactant valley and which inhibits large-amplitude excursions from the TS into the product valley. An analogous barrier was found by Bergsma *et al.*[8(a)] (see pp. 1365–1366 and Fig. 9) in their parabolic model treatment of the frozen-solvent potential-energy function as discussed in the Introduction.

J. Symmetric versus nonsymmetric reactions

Consider the total ensemble-averaged generalized force $F_T[y^\ddagger] = F_g[y^\ddagger] + \langle F\rangle_0$ acting on the reaction coordinate at the TS. By Eq. (3.13) this force vanishes. For symmetric reactions, $\langle F\rangle_0 = 0$ [Eq. (3.32)] and thus the gas-phase and liquid-phase forces $F_g[y^\ddagger]$ and $\langle F\rangle_0$ separately vanish for such reactions. Stated slightly differently, for symmetric reactions the position of the maximum of the gas-phase MERP potential coincides with the position of the minimum of the liquid-phase cage potential [Eq. (3.33b)], $W_c[y]$. Both extrema occur at $y = y^\ddagger$. This guarantees that $W_{MIP}[y]$, defined in Eq. (3.26), has its extremum at the TS in accord with the discussion Sec. III E.

For nonsymmetric reactions $\langle F\rangle_0 \neq 0$ and, therefore, $F_g[y^\ddagger]$ and $\langle F\rangle_0$ do not separately vanish. Rather the force balance condition, Eq. (3.13), implies $F_g[y^\ddagger] = -\langle F\rangle_0$. This difference may be traced to the fact that for nonsymmetric reactions the value of the reaction coordinate at the gas-phase TS, $y^\ddagger_{gas}$, does not coincide with its value $y^\ddagger$ at the liquid-phase TS. (Stated slightly differently, for triatomic $A + BC$ reactions the deformation of the TS geometry which occurs upon solvation changes only the symmetric stretch and bend coordinates, keeping the asymmetric stretch coordinate fixed at zero. For nonsymmetric reactions all three coordinates change upon solvation.) Hence, while $F_g[y^\ddagger_{gas}] = 0$, $F_g[y^\ddagger] = -\langle F\rangle_0 \neq 0$ for nonsymmetric reactions.

An immediate consequence is that the maximum of the gas-phase MERP potential $V_g[y]$ occurs at a point $y^\ddagger_{gas}$ which is shifted from the liquid-phase TS value $y^\ddagger$. One thus requires a corresponding shift in the minimum of the cage potential $W_c[y]$ in order that $W_{MIP}[y]$ retain its extremum at $y = y^\ddagger$.

One finds, in fact, from Eqs. (3.30) and (3.31) that the minimum of $W_c[y]$ occurs for nonsymmetric reactions at $y = y^* - \omega_e^{-2}\tilde{F}^* = \omega_e^{-2}\langle F\rangle_0$ rather than at $y = y^\ddagger = 0$. This minimum occurs in the product valley if $\langle F\rangle_0 > 0$ and in the reactant valley if $\langle F\rangle_0 < 0$. The shift in the minimum reflects the fact that the reaction coordinate is unstable under the liquid-phase force $\langle F\rangle_0$ when it is located at the TS. (This instability is closely related to the fact that the coupled oscillators y and $\tilde{F}$ discussed in Sec. III G are, for nonsymmetric reactions, unstable at $y = \tilde{F} = 0$ but are instead stable at $y = y^*$ and $\tilde{F} = \tilde{F}^*$.)

The discussion of this section may be summarized as follows. For symmetric reactions the extrema of $V_g[y]$, $W_c[y]$, and $W_{MIP}[y]$ coincide at the liquid-phase TS $y^\ddagger = 0$. For nonsymmetric reactions the maximum of $V_g[y]$ is shifted to the gas-phase TS $y^\ddagger_{gas}$ while the minimum of $W_c[y]$ is shifted to $y = \omega_e^{-2}\langle F\rangle_0$. These shifts compensate so that the extremum of $W_{MIP}[y]$ remains at $y^\ddagger = 0$.

K. The parabolic model

The rate-constant results, Eqs. (1.1) and (1.2), quoted in the Introduction are based on the parabolic model for $W_{MIP}[y]$. In this section we briefly discuss this model which is based on the parabolic expansion of $W_{MIP}[y]$ given in Eq. (3.16). With use of Eqs. (2.9), this expansion may be rewritten as

$$W_{MIP}[y] = E_A - \tfrac{1}{2}\omega^2_{MIP}y^2 \quad \text{(parabolic model)}, \tag{3.34}$$

where ω_{MIP} is the parabolic model barrier frequency defined by

$$\omega^2_{MIP} = \omega_g^2 - \omega_e^2, \tag{3.35}$$

with

$$\omega_g^2 = -V_g''[y^\ddagger] \tag{3.36}$$

and with ω_e^2 given by Eq. (3.17a).

Two points concerning the parabolic model should be noted.

(i) Three distinct cases are possible. One may have a parabolic barrier, $\omega^2_{MIP} > 0$, a parabolic well, $\omega^2_{MIP} < 0$, or no parabolic order contribution to $W_{MIP}[y]$, $\omega^2_{MIP} = 0$. [These cases have also been discussed by van der Zwan and Hynes;[19] see, e.g., Figs. 4 and 8 of Ref. 19(a), and by Wilson and co-workers.[8]] We will restrict ourselves in this paper to the case of a parabolic barrier in $W_{MIP}[y]$. That is, we will restrict ourselves to systems which satisfy

$$\omega_g^2 > \omega_e^2 \quad \text{(parabolic barrier)}. \tag{3.37}$$

(ii) We expect that the range of applicability of the parabolic model for the rate constant (see Introduction) is likely to be more restricted for nonsymmetric than for symmetric reactions. We expect the limitations of the model to be particularly severe for strongly exothermic or strongly endothermic reactions.

To see this note that the error in the parabolic approximation to $W_{MIP}[y]$ [Eq. (3.34)] arises completely from the quadratic expansion of the *gas-phase* MERP potential $V_g[y]$. (This follows since the cage potential $W_c[y]$ [Eq. (3.25)] is a quadratic function of y.) However for nonsymmetric reactions and, particularly, for strongly nonthermoneutral reactions, the curvature of the gas-phase MERP potential $V_g[y]$ can change rapidly near the TS,[11] leading to a breakdown of the constant curvature approximation inherent in the parabolic model. (Lee and Hynes[18] have also discussed the limitations of the parabolic model for strongly nonthermal neutral reactions. However, their discussion was based on the potential of mean force rather than the gas phase potential.) As a second point, the parabolic model is conventionally[15] developed as a quadratic fit to the *maximum* of a reactive potential analogous to the quadratic fit to the minimum of a bound potential which is the basis of the harmonic-oscillator approximation. Recall, however (Sec.

III J), that $V_g[y]$ has its maximum at $y = y^{\ddagger}_{gas}$ rather than at $y = y^{\ddagger}$ and that for nonsymmetric reactions $y^{\ddagger}_{gas} \neq y^{\ddagger}$. Thus, for nonsymmetric reactions the parabolic expansion of $V_g[y]$ about $y = y^{\ddagger}$ rather than about its maximum $y = y^{\ddagger}_{gas}$ is an approximation which requires further examination.

IV. THEORETICAL STUDIES OF THE CHLORIDE–METHYL CHLORIDE S_N2 REACTION

Chandrasekhar and co-workers[17] and Wilson and co-workers[8] have recently performed computational studies of the following aqueous S_N2 reaction:

$$Cl^- + CH_3Cl' \rightarrow ClCH_3 + Cl'^-. \quad (4.1)$$

Next we summarize those aspects of the work of these authors which are relevant to the present paper.

A. The quantum chemical and Monte Carlo studies of Chandrasekhar and co-workers

The *gas-phase* MERP potential $E(r_c)$ for the reaction of Eq. (4.1) has been determined by the method of *ab initio* quantum chemical calculation by Chandrasekhar and co-workers.[17] The determination was restricted to collinear Cl, Cl', and C geometries. Chandrasekhar and co-workers give the following parametrization[35] of their computed gas-phase MERP potential:

$$E(r_c) = 30.45 \exp[-(r_c/0.8682)^2] + 192.3/(|r_c| + 1.599)^6 - 140.6/(|r_c| + 1.915)^2, \quad (4.2)$$

where, in accord with Eq. (2.1), $r_c = r_{CCl'} - r_{CCl}$, with r_{CCl} and $r_{CCl'}$ equal, respectively, to the C–Cl and C–Cl' internuclear separations. Note that in Eq. (4.2), r_c is in Å and $E(r_c)$ is in kcal/mol.

Chandrasekhar and co-workers have also performed Monte Carlo (MC) calculations of the liquid-phase contribution to the potential of mean force. The MC simulations were performed for a $Cl^- + CH_3Cl$ system present at infinite dilution in a water-like solvent[17] at a temperature of 25 °C and pressure of 1 atm. By combining these MC results with the quantum chemical results of Eq. (4.2), the potential of mean force evaluated along the gas-phase MERP was determined for the system. Both the gas-phase MERP potential and this potential of mean force curve are plotted in Fig. 1.

B. The molecular-dynamics simulations of Wilson and co-workers

The dynamics of a model aqueous S_N2 reaction designed to mimic the $^{35}Cl^- + CH_3Cl$ (Ref. 35) nucleophilic substitution reaction has been studied by molecular-dynamics (MD) simulation by Wilson and co-workers.[8] These MD simulations assumed a $Cl^- + CH_3Cl$ system present at infinite dilution in a water-like solvent[8] at a temperature of 298 K and mass density of 1 g cm^{-3}. For comparison purposes, the dynamics of 11 other model $A^- + BA$ aqueous nucleophilic substitution reactions were studied by Gertner, Wilson, and Hynes.[8b] These are characterized by values of the gas-phase barrier height and/or "charge switching parameter"[8a] which differ from those of the basic $Cl^- + CH_3Cl$ system. These 12 systems have gas-phase barrier heights, *relative to the ion–dipole minima* (Fig. 1) of 4.9, 13.9, and 31.9 kcal/mol, and thus span a representative range of barrier heights for thermoneutral liquid-phase reactions.

Nine of the twelve S_N2 systems studied, including the basic system, displayed early-time parabolic *barriers*; i.e., satisfied the criterion [see, e.g., Eq. (3.37)] $\omega^2_{MIP} > 0$. In Table I we reproduce, in our notation, some of the quantities computed by MD for these nine systems. These include $\beta^{1/2}(t=0)$, which satisfies the relations [Eqs. (3.27) and (3.28)]

$$\beta^{1/2}(t=0) = [(k_B T)^{-1}\langle \tilde{F}^2\rangle_0]^{1/2} = (\omega_e^2 - \Omega_0^2)^{1/2} \quad (4.3)$$

and the barrier frequencies of $W_{MIP}[y]$, and $W_{PMF}[y]$, respectively, ω_{PMF} and ω_{MIP}. These quantities are basic ingredients required to construct the cage potential $W_c[y,\tilde{F}]$, Eq. (3.33a), and the parabolic model transmission coefficient κ, Eqs. (1.1) and (1.2). Also reproduced in Table I are the average excursions of the asymmetric stretch coordinate Δr_{as} for the nine systems. The Δr_{as} values are very small, in fact smaller than typical root-mean-square vibrational displacements, ranging from 0.013 to 0.030 Å.

TABLE I. Parameters for the model S_N2 systems computed by Wilson and co-workers (Ref. 8).

Model system	Gas-phase barrier height (kcal/mol)	Relative rate of charge switching	Average excursion Δr_{as} (Å)	ω_{PMF} (cm^{-1})	ω_{MIP} (cm^{-1})	$\beta^{1/2}(t=0)$ (cm^{-1})
1	4.9	0.5	0.027	500 ± 6%	190 ± 9%	470 ± 7%
2	4.9	1.0	0.020	860 ± 7%	190 ± 9%	840 ± 7%
3	4.9	2.0	0.023	1730 ± 9%	230 ± 11%	1720 ± 9%
4	13.9	0.5	0.021	640 ± 6%	440 ± 2%	460 ± 12%
5	13.9	1.0	0.020	930 ± 9%	450 ± 2%	820 ± 11%
6	13.9	2.0	0.017	1780 ± 17%	450 ± 4%	1720 ± 18%
7	31.9	0.5	0.022	1040 ± 5%	910 ± 0.4%	510 ± 19%
8	31.9	1.0	0.030	1280 ± 6%	910 ± 0.4%	900 ± 12%
9	31.9	2.0	0.013	1740 ± 7%	910 ± 0.8%	1490 ± 10%

The smallness of the average excursions Δr_{as} makes plausible both the use of the parabolic model for the transmission coefficient κ and the use of the partial-clamping equation of motion, Eqs. (2.6) (which we recall requires the small excursion approximation) to evaluate the friction kernel $\beta(t)$ and other liquid-state quantities required to compute this transmission coefficient. Wilson and co-workers, in fact, find (Table II) that parabolic model transmission coefficient κ, when constructed using the partial-clamping approximation, agrees well for all model systems with the "exact" transmission coefficient κ_{MD} computed from MD trajectories.

C. Construction of the instantaneous potentials

The MD data of Table I, when used in conjunction with the gas-phase MERP potential $E(r_c)$ of Eq. (4.2), in principle, permits construction of the instantaneous potentials $W_{IP}[y,\tilde{F}]$ and $W_{MIP}[y]$ (see Sec. III) for the basic S_N2 system (entry 5 of Table I). For example, from Eq. (3.26) and (3.33b), it follows that for symmetric reactions $W_{MIP}[y]$ takes the following form:

$$W_{MIP}[y] = E_A + V_g[y] - V_g[y^\ddagger] + \tfrac{1}{2}\omega_e^2 y^2. \tag{4.4}$$

Defining $W_{MIP}[r_c]$ by $W_{MIP}[r_c] \equiv W_{MIP}[y]$, one has from Eqs. (2.2), (2.3), (4.2), and (4.4) that for symmetric reactions (for which $x^\ddagger = 0$)

$$W_{MIP}[r_c] = E_A + E(r_c) - E(r_c = 0) + \tfrac{1}{8}\mu_{as}\omega_e^2 r_c^2, \tag{4.5}$$

where, in accord with the discussion of Sec. II C, we have made the identification

$$E(r_c) = V_g[\tfrac{1}{2}(\mu_{as})^{1/2} r_c]. \tag{4.6}$$

The liquid-phase activation energy E_A, as determined by the calculations of Chandrasekhar and co-workers,[17] is

$$E_A = 26.3 \pm 0.5 \text{ kcal/mol} \tag{4.7}$$

in close agreement with the experimental value of $E_A = 26.6$ kcal/mol.[17] Finally, for collinear $Cl^- + CH_3Cl$ configurations $r_{CCl} = -r_{CCl'}$, and thus the mass factor μ_{as} defined in Eq (2.4) reduces to the following form:

$$\mu_{as} = \frac{2M_{Cl}M_{CH_3}}{2M_{Cl} + M_{CH_3}} = 12.35 \text{ amu}, \tag{4.8}$$

where the numerical value in Eq. (4.8) holds for the ^{35}Cl and ^{12}C isotopes.

Given Eqs. (4.2) and (4.5)–(4.8), $W_{MIP}[r_c]$ may be constructed for the basic S_N2 system if ω_e can be determined. Similarly $W_{IP}[r_c,\tilde{F}]$ may be computed from the above equations if ω_e is known via the relationship

$$W_{IP}[r_c,\tilde{F}] = E_A + E(r_c) - E(r_c = 0) + \frac{1}{8}\mu_{as}\omega_e^2\left[r_c - \frac{2\omega_e^{-2}}{(\mu_{as})^{1/2}}\tilde{F}\right]^2 + \frac{1}{2}\frac{\Omega_0^2}{\omega_e^2}\frac{\tilde{F}^2}{\omega_e^2 - \Omega_0^2}. \tag{4.9}$$

Equation (4.9) may be developed from the results of Sec. III following steps analogous to those used to obtain Eq. (4.5).

We next estimate ω_e. We begin with the following expression for ω_{PMF} which follows from Eq. (3.14):

$$\omega_{PMF}^2 = \omega_g^2 - \Omega_0^2, \tag{4.10}$$

where

$$\omega_g^2 = -V_g''[y^\ddagger]. \tag{4.11}$$

If ω_g were known ω_e could be computed from Eqs. (4.3) and (4.10) and the results for ω_{PMF} and $\beta^{1/2}(t=0)$ given in Table I.

To exactly determine ω_g one must know the exact MERP potential $V_g[y]$. Recall (Sec. II C), however, that $V_g[y]$ includes both the effects of kinetic- and potential-energy couplings as well as effects of liquid-phase distortion of the reaction path. In this first treatment, we will ignore these effects. Then, ω_g may be estimated as the parabolic barrier frequency of the gas-phase potential-energy surface of the solute. This has been given for the $Cl^- + CH_3Cl$ system by Bergsma *et al.*[8(a)] as

$$\omega_g = 461 \text{ cm}^{-1}. \tag{4.12}$$

Use of Eq. (4.12) and the most probable results for ω_{PMF} and $\beta^{1/2}(t=0)$ given in Table I yields the following estimate for ω_e:

$$\omega_e \cong 141 \text{ cm}^{-1}. \tag{4.13}$$

$W_{MIP}[r_c]$ may now be computed from Eqs. (4.5) and (4.13), and the other results in this section. This is how the plot of $W_{MIP}[r_c]$ given in Fig. 2 is constructed. To analogously construct $W_{IP}[r_c,\tilde{F}]$ from Eq. (4.9) one additionally requires a value of $\tilde{F}$. The plots in Fig. 3 are constructed with $\tilde{F}$ taken as having the following representative [see Eq. (3.6)] values:

$$\tilde{F} = \pm(\langle\tilde{F}^2\rangle_0)^{1/2} = \pm[k_B T\beta(t=0)]^{1/2}, \tag{4.14}$$

where $T = 298$ K and with $\beta^{1/2}(t=0)$ taken as the most probable value of entry 5 of Table I.

We emphasize that the present procedure for obtaining the instantaneous potentials is subject to considerable uncertainty both because of the approximations made in obtaining ω_g and because of the statistical uncertainties in the MD results. Thus the plots in Figs. 2 and 3 have only qualitative significance. We plan to present a more refined calculation of the instantaneous potential elsewhere.

V. THE PARABOLIC MODEL TRANSMISSION COEFFICIENT

In the Introduction, we discussed the parabolic model formula for the transmission coefficient κ, namely Eqs. (1.1) and (1.2). This transmission coefficient formula is derived in the Appendixes. In this section, we develop the parabolic model equation of motion upon which the analysis in the Appendixes is based and also briefly summarize some results of this analysis. We then use the transmission coefficient formula to interpret the aqueous S_N2 MD results of Wilson and co-workers.[8]

A. The parabolic model equation of motion

The parabolic model equation of motion for the reaction coordinate y takes the following form:

$$\ddot{y}(t) = \omega_{\mathrm{MIP}}^2 y(t) + \int_0^t \Theta(t-\tau)y(\tau)d\tau + \tilde{F}_0(t), \quad (5.1)$$

where the parabolic model barrier frequency ω_{MIP} is given in Eq. (3.35) and where the relaxation function $\Theta(t)$ is defined by

$$\Theta(t) = (k_B T)^{-1}\langle \tilde{F}(t)\tilde{F}\rangle_0. \quad (5.2)$$

Equation (5.1) is derived from our basic equation of motion, Eq. (2.6), using the parabolic approximation to $F_{\mathrm{MIP}}[y]$, namely $F_{\mathrm{MIP}}[y] = -\omega_{\mathrm{MIP}}^2 y$, which follows from the relation $F_{\mathrm{MIP}}[y] = -dW_{\mathrm{MIP}}[y]/dy$, Eq. (3.8), and the parabolic approximation to $W_{\mathrm{MIP}}[y]$, Eq. (3.34). To obtain Eq. (A1) we also used the approximation to the fluctuating force $\tilde{F}_{0(t)}(t)$ given in Eq. (2.8). We next define the normalized velocity autocorrelation function of the reaction coordinate $\dot{\chi}(t)$ by

$$\dot{\chi}(t) = (k_B T)^{-1}\langle \dot{y}(t)\dot{y}\rangle. \quad (5.3)$$

[$\dot{\chi}(t)$ is referred to as normalized since $\dot{\chi}(0) = 1$.] Using the orthogonality relation $\langle \tilde{F}(t)\dot{y}\rangle_0 = 0$, which follows from the definitions of the ensemble average $\langle\cdots\rangle_0$ (Sec. II B) and of fluctuating force $\tilde{F}_0(t)$, Eq. (2.10b), the following equation of motion for $\dot{\chi}(t)$ may be derived from Eq. (5.1):

$$\ddot{\chi}(t) = \omega_{\mathrm{MIP}}^2 \chi(t) + \int_0^t \Theta(t-\tau)\chi(\tau)d\tau. \quad (5.4)$$

B. The velocity autocorrelation function

In Appendix A, we present an analysis of the analytic structure of the velocity response function $\dot{\chi}(z)$. This is defined in terms of the velocity autocorrelation function $\dot{\chi}(t)$ via the Laplace transform relationship[36] $\hat{\dot{\chi}}(z) \equiv \mathcal{L}\dot{\chi}(t)$. This analytic structure is significant since it underlies the unbound character of parabolic model reaction coordinate motion required (Appendix B) for the existence of a nonvanishing parabolic model rate constant.

We show in Appendix A, under the assumption [Eq. (A7)] that the relaxation function $\Theta(t)$ has a discrete spectrum, that the velocity response function $\dot{\chi}(z)$ is analytic except for simple poles. These occur as complex conjugate pairs $\pm i\omega_n$ on the imaginary axis and as a *single* positive and negative pair $\pm x_+$ on the real axis. In contrast, the velocity response function for a bound parabolic solute coordinate [assuming Eq. (A7) holds] has only pure imaginary poles $\pm i\omega_n$.

We further show in Appendix A that the positive real pole x_+, which is the reactive frequency discussed in the Introduction, satisfies the following bounds [these bounds have also been discussed by Gertner, Wilson, and Hynes[8(b)]]:

$$\omega_{\mathrm{MIP}} < x_+ < \omega_{\mathrm{PMF}}, \quad (5.5)$$

where ω_{PMF} is the barrier frequency of the potential of mean force $W_{\mathrm{PMF}}[y]$ given in Eq. (A17). Equation (5.5) places bounds on the transmission coefficient κ.

We additionally show in Appendix A that the velocity autocorrelation function $\dot{\chi}(t)$ for the reaction coordinate takes the following form:

$$\dot{\chi}(t) = \tfrac{1}{2}g_+[\exp(x_+ t) + \exp(-x_+ t)] + \sum_n g_n \cos\omega_n t, \quad (5.6)$$

where g_+ and g_n are positive real constants defined in Eq. (A22). Notice that $\lim_{t\to\infty}\dot{\chi}(t) = \infty$ reflecting the unbound character of reaction coordinate motion. In contrast,[1(a)] for bound parabolic solute degrees of freedom $\lim_{t\to\infty}\dot{\chi}(t) = 0$.

C. Interpretation of the S_N2 results of Wilson and coworkers

Next, we provide some further discussion of the MD simulation results of Wilson and co-workers.[8] We will see that these results are in accord with the concepts of our theory[1] as summarized in the Introduction. In Table II we reproduce some of the results of Gertner, Wilson, and Hynes[8(b)] for the nine model systems listed in Table I. We begin with our basic expression for the transmission coefficient, Eq. (1.1),

TABLE II. Transmission coefficients and other parameters for the model S_N2 systems computed by Wilson and co-workers (Ref. 8).

Model system	Gas-phase barrier height (kcal/mol)	x_+	ω_{PMF} (cm^{-1})	ω_{MIP} (cm^{-1})	κ_0	κ_{MD}	κ
1	4.9	280	500 ± 6%	190 ± 9%	0.37 ± 0.03	0.49 ± 0.04	0.56 ± 0.04
2	4.9	370	860 ± 7%	190 ± 9%	0.22 ± 0.02	0.43 ± 0.05	0.43 ± 0.04
3	4.9	580	1730 ± 9%	230 ± 11%	0.14 ± 0.01	0.32 ± 0.05	0.33 ± 0.04
4	13.9	470	640 ± 6%	440 ± 2%	0.69 ± 0.03	0.71 ± 0.04	0.74 ± 0.07
5	13.9	530	930 ± 9%	450 ± 2%	0.48 ± 0.03	0.54 ± 0.04	0.57 ± 0.08
6	13.9	650	1780 ± 17%	450 ± 4%	0.25 ± 0.03	0.40 ± 0.05	0.37 ± 0.10
7	31.9	910	1040 ± 5%	910 ± 0.4%	0.87 ± 0.02	0.90 ± 0.02	0.88 ± 0.08
8	31.9	930	1280 ± 6%	910 ± 0.4%	0.71 ± 0.02	0.75 ± 0.03	0.73 ± 0.05
9	31.9	990	1740 ± 7%	910 ± 0.8%	0.52 ± 0.02	0.50 ± 0.04	0.57 ± 0.05

$$\kappa = x_+ / \omega_{\mathrm{PMF}}, \tag{5.7}$$

where the reactive frequency x_+ is determined by the self-consistent equation (1.2). In the limit $\omega_{\mathrm{MIP}}^{-2}\Theta(x_+) \ll 1$, this self-consistent equation reduces to the following form:

$$x_+ \doteq \omega_{\mathrm{MIP}} + \tfrac{1}{2}\omega_{\mathrm{MIP}}^{-1}\hat{\Theta}(\omega_{\mathrm{MIP}}). \tag{5.8}$$

The result $x_+ = \omega_{\mathrm{MIP}}$ gives the reactive frequency in the rigid-cage or frozen-solvent limit. The full result, Eq. (5.8), corrects this zeroth-order limit for the effects of relaxation of the environment (i.e., the zq degrees of freedom) in response to the motion of the reaction coordinate. Consequently, Eq. (5.7) provides a useful approximation if the environmental relaxation is sufficiently weak.

Equation (5.8) predicts that x_+, and hence the barrier passage velocity, should "track" with the sharpness of the barrier of $W_{\mathrm{MIP}}[y]$ rather than (as is usually assumed) with that of $W_{\mathrm{PMF}}[y]$. This is in accord with the discussion in the Introduction.

The MD results for x_+, computed using the partial-clamping model, are listed in Table II. These results clearly show that the variation of x_+ over the nine model aqueous S_N2 systems is governed by ω_{MIP} rather than by ω_{PMF}. For example, for the three high barrier systems (gas-phase barrier heights of 31.9 kcal/mol) the values of both the reactive frequency x_+ and the barrier frequency ω_{MIP} are weak functions of the charge switching parameter. Specifically, x_+ is equal to, respectively, 910, 930, and 990 cm^{-1} for the three charge switching cases while $\omega_{\mathrm{MIP}} = 910\ \mathrm{cm}^{-1}$ for all three cases. Notice that $x_+ \approx \omega_{\mathrm{MIP}}$ in accord with the frozen-solvent limit of Eq. (5.8). The barrier frequency ω_{PMF}, in contrast, is a strong function of the charge switching parameter and takes on the values ω_{PMF} equal to, respectively, 1040, 1280, and 1740 cm^{-1}.

Also, the small increase of x_+ with switching parameter for the 31.9 kcal/mol systems can be qualitatively understood using Eq. (5.8). As the charge switching parameter increases, the coupling of the reaction coordinate to the environment, measured by $\beta^{1/2}(t=0)$ (Table I), also increases leading to an increased environmental relaxation contribution to x_+.

The same trends are evident for the lower barriers. For a gas-phase barrier height of 13.9 kcal/mol, x_+ ranges from 470 to 650 cm^{-1}, while ω_{MIP} and ω_{PMF} range, respectively, from 440 to 450 cm^{-1} and from 640 to 1780 cm^{-1}. Similarly, for the low barrier case of 4.9 kcal/mol one has the ranges $x_+ = 280$–$580\ \mathrm{cm}^{-1}$, $\omega_{\mathrm{MIP}} = 190$–$230\ \mathrm{cm}^{-1}$, while $\omega_{\mathrm{PMF}} = 500$–$1730\ \mathrm{cm}^{-1}$.

Notice that the importance of environmental relaxation increases as the gas-phase barrier heights decrease. Thus, as expected, the physics discussed in the Introduction manifests itself most distinctly for the higher activation barriers. However, even for the 4.9 kcal/mol barrier $W_{\mathrm{MIP}}[y]$ provides a much better zeroth-order potential for reaction coordinate dynamics than $W_{\mathrm{PMF}}[y]$.

Comparison of Eqs. (5.7) and (5.8) yields the following approximate result for the transmission coefficient κ [Eq. (1.4)]:

$$\kappa \doteq \omega_{\mathrm{PMF}}^{-1}(\omega_{\mathrm{MIP}} + \tfrac{1}{2}\omega_{\mathrm{MIP}}^{-1}\hat{\Theta}[\omega_{\mathrm{MIP}}]). \tag{5.9}$$

The trends in x_+ just discussed reflect themselves as trends in the transmission coefficients. This is evident from Table II where we list the frozen-solvent result for the transmission coefficient $\kappa_0 = \omega_{\mathrm{PMF}}^{-1}\omega_{\mathrm{MIP}}$, the exact result κ_{MD} computed by MD simulation of the reactive dynamics, and the parabolic model result κ. The frozen-solvent result is most accurate for high barriers and weak coupling. Environmental relaxation becomes increasingly important for low barriers and strong coupling. It is interesting to note, as emphasized by Gertner, Wilson, and Hynes,[8(b)] that the parabolic model result for κ is in very good accord with the exact result κ_{MD} for all S_N2 model systems.

VI. SUMMARY AND DISCUSSION

In the Introduction we discussed certain physical principles[1-7] which are important for the interpretation of dynamic solvent effects on chemical reactions and related molecular phenomena. These principles derive from generic rather than specific features of the underlying molecular interactions and are, therefore, expected to apply widely in liquid-phase chemistry.

In brief, very often the nature of the solute motions which occur on realistic potential-energy surfaces[11] is such that the solvent following of these motions is highly imperfect relative to its following of the more familiar[13] thermal solute motions. Thermodynamic equilibrium between the solute and the solvent is, therefore, not even approximately maintained during a liquid-phase event. Rather, forces which act to restore equilibrium play a critical role in influencing the dynamics of both the solute and the solvent. These forces are ignored in traditional "equilibrium solvation" descriptions[14] of liquid-phase reactions.

In this paper, we developed the implications of these general principles for the specific problem of liquid-phase activated barrier crossing. We focused, in particular, on the early-time regime (times short compared to the relaxation time of $\langle \tilde{F}(t)\tilde{F}\rangle_0$) in which the solvent is nearly "frozen." This regime was found to be important for the determination of the rate constant in the simulations of model S_N2 reactions due to Wilson and co-workers.[8] In the early-time regime, the nonequilibrium effects produce cage confinement forces (see Figs. 2 and 3) which can yield oscillatory solute motions that differ markedly from gas-phase motions. Such effects are evident in the molecular-dynamics (MD) studies of the $Cl^- + CH_3Cl$ substitution reaction due to Bergsma *et al.*[8(a)] These authors find that barrier recrossing is significantly more prominent in aqueous solution ($\sim 63\%$ recrossing) than in the gas phase ($\sim 16\%$ recrossing).

The work in this paper is based on a generalized Langevin equation of motion which governs the dynamics of the reaction coordinate y of the solute system. This equation of motion is [$\beta = (k_B T)^{-1}$]

$$\ddot{y}(t) = F_{\mathrm{MIP}}[y(t)] + \int_0^t \langle \tilde{F}(t-\tau)\dot{\tilde{F}}_0\rangle_0 y(\tau)\,d\tau + \tilde{F}_0(t). \tag{6.1}$$

The equation of motion Eq. (6.1) naturally represents the physics of the early-time regime. Specifically, $F_{\mathrm{MIP}}[y]$ is the

ensemble-averaged force which would be experienced by the reaction coordinate if the time for the reaction were infinitely short. The integral kernel term corrects this frozen-solvent limit for the ensemble-averaged effects of environmental relaxation. The fluctuating force $\tilde{F}_0(t)$ accounts for deviations from the ensemble-averaged description due to environmental fluctuations.

We begin our synopsis of the work in this paper with a discussion of the instantaneous potential $W_{\rm IP}[y,\tilde{F}]$ introduced in Sec. III and plotted in Figs. 2 and 3. This potential, which may be developed from the $t\to 0$ limit of Eq. (6.1), governs reaction coordinate dynamics in the extreme short-time-scale limit. In fact, the main features of the full spectrum of solvent effects on early-time reaction dynamics may be inferred from the form of the instantaneous potential. For example, both the early-time barrier recrossing processes and their dependence on static environmental fluctuations are expected from the form of $W_{\rm IP}[y,\tilde{F}]$.

To illustrate this point, we next discuss certain gross effects of the environmental fluctuations. These enter our treatment through the dependence of $W_{\rm IP}[y,\tilde{F}]$ on the initial value of the fluctuating force $\tilde{F}\equiv\tilde{F}_0[t=0]$. For $\tilde{F}<0$ one has a reactant-like fluctuation while for $\tilde{F}>0$ one has a product-like fluctuation. (This terminology is qualitative; see Sec. III I.) The effects of these fluctuations on $W_{\rm IP}[y,\tilde{F}]$ are shown in Fig. 3. There $W_{\rm IP}[y,\tilde{F}]$ is plotted for the aqueous $Cl^- + CH_3Cl$ system for a representative reactant-like [Fig. 3(a)] and product-like [Fig. 3(b)] fluctuation $\tilde{F}$. $W_{\rm MIP}[y] = W_{\rm IP}[y,\tilde{F}=0]$ is plotted for the same system in Fig. 2. The plots of $W_{\rm IP}[y,\tilde{F}]$ in Fig. 3 show that reactant-like fluctuations are expected to *promote* barrier recrossing processes of the following type: Transition state→products→transition state→reactants. Product-like fluctuations are expected to *impede* such processes. These expectations are in accord with the MD results of Wilson and co-workers.[8] They find, in fact, that, barrier recrossing from products to reactants occurred *only* in the presence of reactant-like static solvent density fluctuations.

We next turn to the parabolic model rate constant. The physics of the early-time regime has implications for the form of the parabolic model transmission coefficient κ [see Eq. (1.4)], for its variation with the solute–solvent system and thermodynamic state (see Sec. V C), and for its range of validity.

We will discuss here questions of validity. The parabolic model formula for κ works well[8(b)] for the model S_N2 systems of Wilson and co-workers. Despite this, the analysis in this paper suggests certain limitations of the parabolic model. First, one expects the model to have a more restricted range of application for nonsymmetric than for symmetric reactions. We expect that the limitations of the model will be particularly severe for reactions which are strongly exothermic or strongly endothermic in the *gas phase*. This follows since the error in the model arises solely from the quadratic expansion of the gas-phase potential. (This is true given our assumption (Sec. III) of a *harmonic* cage potential $W_c[y,\tilde{F}]$.) However, for nonthermoneutral reactions, particularly strongly endothermic or exothermic reactions, the curvature of $V_g[y]$ can change rapidly near the transition state,[11] rendering the constant curvature assumption inherent in the parabolic model questionable.

Second, it is evident from the plots of $W_{\rm MIP}[y]$ and $W_{\rm IP}[y,\tilde{F}]$ given in Figs. 2 and 3 that the parabolic model predicts no product→reactant barrier recrossing except in the presence of a reactant-like environmental fluctuation. Thus if such barrier recrossing is found in the presence of product-like fluctuations or in the presence of a symmetric environment, this is a diagnostic indicating breakdown of the parabolic model. This diagnostic is, however, only strictly valid in the extreme short-time-scale limit.

Finally, we wish to emphasize that a number of assumptions have been made in the present treatment. Our analysis, for example, is based on an effective[5] one-dimensional description of the reaction coordinate dynamics rather than an explicitly multidimensional treatment of the solute dynamics. Additionally, we have utilized harmonic (Sec. III G) rather than anharmonic cage potentials in accord with our assumption (Sec. II B) of small reaction coordinate excursions. Our conclusions, including those concerning the validity of the parabolic model, may require modification when a more refined treatment which lifts these and other restrictions is developed. We hope to present such a refined treatment elsewhere.

ACKNOWLEDGMENTS

We wish to thank Francis Patron for many helpful discussions. Support of this work by the National Science Foundation under Grant No. CHE-8803938 is gratefully acknowledged. R. Muralidhar acknowledges financial support from the Chemical Engineering Department of Purdue University.

APPENDIX A: ANALYTIC STRUCTURE OF THE VELOCITY RESPONSE FUNCTION

To derive the expression for the transmission coefficient given in Eqs. (1.1) and (1.2), we require the $t\to\infty$ limit of the normalized velocity autocorrelation function $\dot{\chi}(t)$ [Eq. (5.3)] of the reaction coordinate y. This limit is determined by the form of the Laplace transform[36] $\hat{\dot{\chi}}(z)$ defined by

$$\hat{\dot{\chi}}(z) = \mathcal{L}\dot{\chi}(t) \equiv \int_0^\infty \exp(-zt)\dot{\chi}(t)dt. \tag{A1}$$

For bound solute degrees of freedom [assuming a discrete spectrum as in Eq. (A7)], $\hat{\dot{\chi}}(z)$ is analytic except for simple poles occurring in complex conjugate pairs on the imaginary axis.[1(a)] For the reaction coordinate y, a different analytic structure is expected reflecting the unbound character of reaction coordinate motion and this is derived in this appendix. [This derivation provides a proof of the existence of a single reactive root of $\hat{\dot{\chi}}(z)$. In earlier work (see, e.g., Refs. 8 and 18, and references therein), the existence of the reactive root has been assumed without proof.]

We begin by noting that within the parabolic model for $W_{\rm MIP}(y)$, $\hat{\chi}(z) = \mathcal{L}\chi(t)$ may be expressed as

$$\hat{\chi}(z) = [z^2 - \omega_{\rm MIP}^2 - \hat{\Theta}(z)]^{-1}, \tag{A2}$$

where $\hat{\Theta}(z) = \mathcal{L}\Theta(t)$. Equation (A2) may be readily de-

rived from the parabolic model equation of motion for $\dot{\chi}(t)$, Eq. (5.4), following steps outlined elsewhere.[1(a)] Rearrangement of Eq. (A2) yields the following form for $\hat{\chi}(z) = z\hat{\chi}(z)$:

$$\hat{\chi}(z) = \tfrac{1}{2}[\hat{G}_+^{-1}(z) + \hat{G}_-^{-1}(z)], \tag{A3}$$

where

$$\hat{G}_+(z) = z - \hat{F}(z) \quad \text{and} \quad \hat{G}_-(z) = z + \hat{F}(z) \tag{A4}$$

with

$$\hat{F}(z) = [\omega_{\mathrm{MIP}}^2 + \hat{\Theta}(z)]^{1/2}. \tag{A5}$$

We next examine the analytic structure of $\hat{\Theta}(z)$. We first note that since $\langle \tilde{F}(t)\tilde{F}\rangle_0$ is computed using the partial-clamping constraint, it is free of contributions from the reactive component of the solute motion. Thus $\Theta(t)$ is expected to have an analytic structure identical to that for the corresponding response functions of bound solute degrees of freedom. Specifically, we expect $\hat{\Theta}(z)$ to have an exact integral representation of the form[1(a)]

$$\hat{\Theta}(z) = \int_0^\infty \frac{\sigma(\omega)d\omega}{z^2 + \omega^2}, \tag{A6}$$

where $\sigma(\omega) \geqslant 0$. [Equation (A6) is equivalent to assuming the fluctuating force $\tilde{F}_0(t)$ has a Fourier integral representation.] The subsequent analysis is considerably simplified if one assumes a discrete spectrum $\sigma(\omega)$, i.e., we assume

$$\sigma(\omega) = \sum_n \sigma_n \delta(\omega - \Omega_n), \tag{A7}$$

where

$$\sigma_n \geqslant 0. \tag{A8}$$

For the case of a discrete spectrum, Eq. (A6) becomes

$$\hat{\Theta}(z) = \sum_n \sigma_n/(z^2 + \Omega_n^2). \tag{A9}$$

We will show that given Eq. (A9) $\hat{\chi}(z)$ has only isolated simple poles which we denote by $z_{\pm n}$. These poles [see Eq. (A3)] coincide with the zeroes of $G_\pm(z)$, i.e.,

$$G_+(z_{+n}) = 0 \quad \text{and} \quad G_-(z_{-n}) = 0. \tag{A10}$$

Using Eqs. (A4) and (A5), Eqs. (A10) may be rewritten as

$$z_{+n} = \hat{F}(z_{+n}) = +[\omega_{\mathrm{MIP}}^2 + \hat{\Theta}(z_{+n})]^{1/2} \tag{A11a}$$

and

$$z_{-n} = -\hat{F}(z_{-n}) = -[\omega_{\mathrm{MIP}}^2 + \hat{\Theta}(z_{-n})]^{1/2}. \tag{A11b}$$

Thus the pole positions $z_{\pm n}$ may be determined as the roots of the self-consistent equations, Eqs. (A11).

We now derive the general properties of these roots. We first note that the roots $z_{\pm n}$ cannot coincide with the poles $\pm i\Omega_n$ [see Eq. (A9)] of $\hat{\Theta}(z)$ since Eqs. (A11) are undefined at $z = \pm i\Omega_n$. We next show that the roots occur as positive and negative pairs, namely

$$z_{-n} = -z_{+n}. \tag{A12}$$

Equation (A12) follows from the evenness [Eqs. (A5) and (A9)] of $\hat{F}(z)$. Specifically, writing Eq. (A11a) as $-z_{+n} = -\hat{F}(z_{+n}) = -\hat{F}(-z_{+n})$ and then comparing with Eq. (A11b) yields Eq. (A12).

We next show that the roots $z_{\pm n}$ are either pure real or pure imaginary. This may be seen by squaring either of Eqs. (A11) to yield $z^2 = \omega_{\mathrm{MIP}}^2 + \hat{\Theta}(z)$. Setting $z = x + i\omega$ in this equation and taking its imaginary part yields

$$2x\omega = \mathrm{Im}\,\hat{\Theta}(x + i\omega)$$

$$= -2x\omega \sum_n \frac{\sigma_n}{(x^2 - \omega^2 + \Omega_n^2)^2 + 4x^2\omega^2}, \tag{A13}$$

where we have used Eq. (A9). Since $\sigma_n \geqslant 0$, the sum on the right-hand side of Eq. (A13) is positive. Thus the right-hand side of Eq. (A13) has the sign of $-2x\omega$. The left-hand side has the opposite sign. Thus Eq. (A13) is correct only if $2x\omega = 0$. That is, the solutions of Eqs. (A11) are either pure real ($\omega = 0$) or pure imaginary ($x = 0$).

We next show that there are only two real solutions which we denote by x_+ and $x_- = -x_+$. Given Eq. (A12), we need to prove the existence of a single positive solution to establish that only two real solutions occur. We rewrite Eq. (A11a) for $z_{+n} = x_+$ as

$$x_+^2 = F^2(x_+) = \omega_{\mathrm{MIP}}^2 + \hat{\Theta}(x_+)$$

$$= \omega_{\mathrm{MIP}}^2 + \sum_n \frac{\sigma_n}{x_+^2 + \Omega_n^2}, \tag{A14}$$

where we have used Eq. (A9). From Eq. (A14), it is evident that for $x > 0$, $F^2(x)$ is a monotonically decreasing positive function which approaches the asymptotic limit ω_{MIP}^2 as $x \to \infty$. In contrast, x^2 is a monotonically increasing positive function for $x > 0$. Moreover, $x^2 < F^2(x)$ as $x \to 0$ and $x^2 > F^2(x)$ as $x \to \infty$. Thus x^2 and $F(x)$ intersect only once giving rise to a single root $x_+ > 0$.

We next put bounds on the root x_+. We begin by noting that from Eq. (5.2) it follows that

$$\hat{\Theta}(z) = (k_B T)^{-1}\langle \tilde{F}^2\rangle_0 - z\hat{\beta}(z), \tag{A15}$$

where $\hat{\beta}(z) = \mathscr{L}\beta(t)$ with $\beta(t)$ defined in Eq. (3.27). Evaluating Eq. (A15) at $z = 0$ and using Eq. (3.28) yields

$$\hat{\Theta}(z = 0) = \omega_e^2 - \Omega_0^2 > 0. \tag{A16}$$

From Eqs. (A5) and (A16) and the definition $\omega_{\mathrm{MIP}}^2 = \omega_g^2 - \omega_e^2$ it follows that $F^2(x = 0) = \omega_g^2 - \Omega_0^2$. Also [Eq. (A14)], $\lim_{x \to \infty} F^2(x) = \omega_{\mathrm{MIP}}^2$. Thus by Eq. (A14), x_+ occurs between $\omega_{\mathrm{MIP}} = (\omega_g^2 - \omega_e^2)^{1/2}$ and $(\omega_g^2 - \Omega_0^2)^{1/2}$. Moreover, since $\omega_e > \Omega_0$ by Eq. (A16) we have the bounds $\omega_{\mathrm{MIP}} < x_+ < (\omega_g^2 - \Omega_0^2)^{1/2}$. However, the barrier frequency of the potential of mean force curve ω_{PMF} is given by [Eq. (4.10)]

$$\omega_{\mathrm{PMF}}^2 = \omega_g^2 - \Omega_0^2. \tag{A17}$$

Thus we have established the following bounds on x_+:

$$\omega_{\mathrm{MIP}} < x_+ < \omega_{\mathrm{PMF}}. \tag{A18}$$

We next turn to the determination of $\dot{\chi}(t) = \mathscr{L}^{-1}\hat{\chi}(z)$. We first note that functions $G_\pm(z)$ are analytic at $z = z_{\pm n}$. This follows by evaluating the derivatives $G'_\pm(z_{\pm n})$ using Eqs. (A4), (A5), (A9), and (A11) to yield

$$G'_{\pm}(z_{\pm n}) = 1 - \frac{1}{2}\frac{\hat{\Theta}'(z_{\pm n})}{z_{\pm n}} = 1 + \sum_n \frac{\sigma_n}{(z^2_{\pm n} + \Omega_n^2)^2}. \tag{A19}$$

Since, as discussed above, the $z_{\pm n}$ do not coincide with the poles $\pm i\Omega_n$ of $\hat{\Theta}(z)$, the derivatives $G'_{\pm}(z_{\pm n})$ exist and, hence, the functions $G_{\pm}(z)$ are analytic at $z = z_{\pm n}$. Thus Taylor-series expansions about $z = z_{\pm n}$ can be made. Since $G_{\pm}(z_{\pm n}) = 0$ [Eq. (A10)] these Taylor series take the following form near $z = z_{\pm n}$:

$$\hat{G}_{\pm}(z) \doteq \hat{G}'_{\pm}(z_{\pm n})(z - z_{\pm n}). \tag{A20}$$

Given Eq. (A20), it follows that to within an entire function which may be shown to vanish Eq. (A3) may be written as

$$\hat{\chi}(z) = \frac{1}{2}\sum_n \{[G'_+(z_{+n})]^{-1}(z - z_{+n})^{-1} + [G'_-(z_{-n})]^{-1}(z - z_{-n})^{-1}\}. \tag{A21}$$

Recalling [Eq. (A12)] that $z_{-n} = -z_{+n}$, it follows from Eq. (A19) that

$$G'_-(z_{-n}) = G'_+(z_{+n}) \equiv g_n^{-1}. \tag{A22}$$

Also, from Eq. (A19) it follows that $G'_{\pm}(z_{\pm n})$ is positive real on either the real or the imaginary axes. Thus it follows from Eq. (A22) that for the positive real root

$$g_+ \equiv g_n > 0, \tag{A23a}$$

while for the pure imaginary roots

$$g_n > 0. \tag{A23b}$$

Finally, using Eqs. (A12) and (A21)–(A22), one has

$$\hat{\chi}(z) = z\hat{\chi}(z) = \frac{1}{2}g_+[(z - x_+)^{-1} + (z + x_+)^{-1}] + \frac{1}{2}\sum_n g_n[(z - i\omega_n)^{-1} + (z + i\omega_n)^{-1}], \tag{A24}$$

where we have separated out the contributions of the real and imaginary roots. Laplace inversion of Eq. (A24) then yields the following form for the normalized velocity autocorrelation function $\dot{\chi}(t)$:

$$\dot{\chi}(t) = \frac{1}{2}g_+[\exp(x_+ t) + \exp(-x_+ t)] + \sum_n g_n \cos\omega_n t. \tag{A25}$$

APPENDIX B: DERIVATION OF THE TRANSMISSION COEFFICIENT FORMULA

In this Appendix, we derive the formula for the transmission coefficient κ given in Eqs. (1.1) and (1.2). We utilize an adaptation of a pedagogically valuable method recently described by Gertner, Wilson, and Hynes.[8(b)] This adaptation lifts the restriction of a harmonic solvent linearly coupled to the reaction coordinate made by Gertner, Wilson, and Hynes,[8(b)] and replaces it by the assumption that the fluctuating force $\tilde{F}_0(t)$ may be modeled by Gaussian noise. We begin by noting that the solution of the parabolic model equation of motion Eq. (5.1) yields the following result for the trajectory $y(t)$ of the reaction coordinate:

$$y(t) = \chi(t)\dot{y} + \dot{\chi}(t)y + \int_0^t \chi(t - \tau)\tilde{F}_0(\tau)d\tau, \tag{B1}$$

where $\dot{y}$ and y are the initial conditions and where $\dot{\chi}(t)$ is the normalized velocity autocorrelation function defined in Eq. (5.3).

We mentioned in Sec. II that the equilibrium rate constant may be computed as a canonical ensemble average over all solute trajectories which originate from a TS ensemble geometry.[21] This condition is enforced within the framework of the present one-dimensional description by setting $y(t = 0) = y = y^{\ddagger} = 0$. Equation (B1) then simplifies to

$$y(t) = \chi(t)\dot{y} + Y(t), \tag{B2}$$

where

$$Y(t) = \int_0^t \chi(t - \tau)\tilde{F}_0(\tau)d\tau = \mathcal{L}^{-1}[\chi(z)\hat{\tilde{F}}_0(z)]. \tag{B3}$$

The following form for $\chi(t)$ may be computed by integration of Eq. (A25):

$$\chi(t) = \tfrac{1}{2}g_+ x_+^{-1}[\exp(x_+ t) - \exp(-x_+ t)] + \sum_n g_n \omega_n^{-1}\sin\omega_n t. \tag{B4}$$

To obtain Eq. (B4) we have used the initial condition $\chi(0) = 0$ which follows by setting $t = 0$ in Eq. (B2) and using $y(t = 0) = Y(t = 0) = 0$. The function $Y(t)$ may be computed by Laplace inversion of Eq. (B3) using Eq. (A24) and the fact that $\hat{\tilde{F}}_0(z)$ may be taken as an even function of z [since $\tilde{F}_0(t)$ may be taken as an even function of t]. This yields

$$Y(t) = \tfrac{1}{2}g_+ x_+^{-1}[\exp(x_+ t) - \exp(-x_+ t)]\hat{\tilde{F}}_0(x_+) + \sum_n g_n \omega_n^{-1}\sin\omega_n t\hat{\tilde{F}}_0(i\omega_n). \tag{B5}$$

To compute the transmission coefficient we require the $t \to +\infty$ limit of $y(t)$. Comparison of Eqs. (B2) and (B4) and (B5) shows that this limit depends only on the positive real root x_+ and, in fact, is given by

$$\lim_{t\to\infty} y(t) = \tfrac{1}{2}g_+ x_+^{-1}\exp(x_+ t)[\dot{y} + \hat{\tilde{F}}_0(x_+)]. \tag{B6}$$

We next discuss the criterion for a successful reactive attempt. For such an attempt $\lim_{t\to\infty} y(t) = +\infty$. Since $x_+ > 0$ and since $g_+ > 0$ [Eq. (A23a)], it is evident from Eq. (B6) that this criterion is

$$\dot{y} > -\hat{\tilde{F}}_0(x_+). \tag{B7}$$

Given Eq. (B7) we may construct the transmission coefficient κ from the following expression:

$$\kappa = \frac{\int_{\dot{y} > -\hat{\tilde{F}}_0(x_+)} d\dot{y}\, d\hat{\tilde{F}}_0(x_+)\dot{y}P_y[\dot{y}]P_F[\hat{\tilde{F}}_0(x_+)]}{\int_{\dot{y}>0} d\dot{y}\, d\hat{\tilde{F}}_0(x_+)\dot{y}P_y[\dot{y}]P_F[\hat{\tilde{F}}_0(x_+)]}, \tag{B8}$$

where P_y and P_F are, respectively, the probability distribution functions (PDF) for $\dot{y}$ and $\hat{\tilde{F}}_0(x_+)$. Equation (B8) is a valid expression for κ since its numerator is proportional to

the total flux which satisfies the reactive criterion Eq. (B7), while its denominator is proportional to the flux which would react if the transition-state-theory criterion for reaction, $\dot{y}>0$, held.

To evaluate Eq. (B8) we require the PDF's P_y and P_F. P_y is the Boltzmann distribution

$$P_y[\dot{y}] = [2\pi\langle\dot{y}^2\rangle]^{-1/2}\exp\left(-\frac{1}{2}\frac{\dot{y}^2}{\langle\dot{y}^2\rangle}\right), \tag{B9}$$

where

$$\langle\dot{y}^2\rangle = k_B T. \tag{B10}$$

To obtain the PDF P_F we assume that the fluctuating force $\tilde{F}_0(t)$ is a Gaussian random process. Then it follows that

$$P_F[\hat{\tilde{F}}_0(x_+)] = [2\pi\langle\hat{\tilde{F}}_0^2(x_+)\rangle_0]^{-1/2} \times\exp\left[-\frac{1}{2}\frac{\hat{\tilde{F}}_0^2(x_+)}{\langle\hat{\tilde{F}}^2(x_+)\rangle_0}\right]. \tag{B11}$$

Because of the Gaussian character of P_y and P_F the integrals in Eq. (B8) are tractable. A brief calculation for the numerator N of Eq. (B8) yields

$$N = \left(\frac{\langle\dot{y}^2\rangle}{2\pi}\right)^{1/2}\left[\frac{\langle\dot{y}^2\rangle}{\langle\dot{y}^2\rangle + \langle\hat{\tilde{F}}^2(x_+)\rangle_0}\right]. \tag{B12}$$

Similarly, for the denominator D one has that

$$D = \left(\frac{\langle\dot{y}^2\rangle}{2\pi}\right)^{1/2}. \tag{B13}$$

Thus $\kappa = D^{-1}N$ takes the form

$$\kappa = \left[\frac{\langle\dot{y}^2\rangle}{\langle\dot{y}^2\rangle + \langle\hat{\tilde{F}}^2(x_+)\rangle_0}\right]^{1/2}. \tag{B14}$$

To complete the calculation we must determine $\langle\hat{\tilde{F}}^2(x_+)\rangle_0$. Since $\hat{\tilde{F}}_0(z) = \mathcal{L}\tilde{F}_0(t) = \int_0^\infty \exp(-zt)\tilde{F}_0(t)dt$, it follows that

$$\langle\hat{\tilde{F}}^2(z)\rangle_0 = \int_0^\infty \exp(-zt)dt\int_0^\infty \exp(-zt') \times\langle\tilde{F}(t)\tilde{F}(t')\rangle_0 dt'. \tag{B15}$$

However, by Eq. (3.27), $\langle\tilde{F}(t)\tilde{F}(t')\rangle_0 = k_B T\beta(t-t')$. Using this result and the evenness of $\beta(t)$, Eq. (B15) may be evaluated. A brief calculation yields

$$\langle\hat{\tilde{F}}^2(z)\rangle_0 = k_B T z^{-1}\hat{\beta}(z). \tag{B16}$$

Comparison of Eqs. (B10), (B14), and (B16) yields

$$\kappa = \left[\frac{x_+^2}{x_+^2 + x_+\beta(x_+)}\right]^{1/2}. \tag{B17}$$

We next return to Eq. (A11a), which we rewrite for $x_+ = z_{+n}$ as

$$x_+^2 = \omega_{\mathrm{MIP}}^2 + \hat{\Theta}(x_+) = \omega_g^2 - \omega_e^2 + \hat{\Theta}(x_+), \tag{B18}$$

where we have used Eq. (3.35) to obtain the final form of Eq. (B18). However, comparison of Eqs. (3.28) and Eq. (A15) yields the following form for $\hat{\Theta}(x_+)$:

$$\hat{\Theta}(x_+) = \omega_e^2 - \Omega_0^2 - x_+\beta(x_+). \tag{B19}$$

Combining Eqs. (A17), (B18), and (B19) then yields

$$x_+^2 = \omega_{\mathrm{PMF}}^2 - x_+\beta(x_+). \tag{B20}$$

Finally, combining Eqs. (B17) and (B20) yields

$$\kappa = x_+/\omega_{\mathrm{PMF}}, \tag{B21}$$

where x_+ is given by

$$x_+ = [\omega_{\mathrm{MIP}}^2 + \hat{\Theta}(x_+)]^{1/2}. \tag{B22}$$

Equations (B21) and (B22) are the required results for the transmission coefficient κ, Eqs. (1.1) and (1.2).

[1] (a) For a rigorous development of our theory of solution reaction dynamics see S. A. Adelman, Adv. Chem. Phys. **53**, 61 (1983). (b) S. A. Adelman, J. Chem. Phys. **71**, 4471 (1979). (c) Our work emerged from an early analysis of gas–solid energy transfer. See B. J. Garrison and S. A. Adelman, Surf. Sci. **66**, 253 (1977). (d) For a synopsis of the physical concepts, see S. A. Adelman, J. Stat. Phys. **42**, 37 (1986). (e) For a detailed description of the concepts, see S. A. Adelman, Rev. Chem. Intermed. **8**, 321 (1987).

[2] For applications to molecular iodine photolysis, see C. L. Brooks III, M. W. Balk, and S. A. Adelman, J. Chem. Phys. **79**, 784 (1983); M. W. Balk, C. L. Brooks III, and S. A. Adelman, *ibid.* **79**, 804 (1983).

[3] For applications to activated barrier crossing and superionic conduction, see M. Olson and S. A. Adelman, J. Chem. Phys. **83**, 1865 (1985).

[4] For a theory of the frequency spectrum of molecular solvents, see S. A. Adelman and M. W. Balk, J. Chem. Phys. **82**, 4641 (1985). For an extension to molecular solvents, see S. A. Adelman and M. W. Balk, J. Chem. Phys. **84**, 1752 (1986).

[5] The partial clamping theory is developed in S. A. Adelman, J. Chem. Phys. **81**, 2776 (1984). The theory is refined and extended to molecular solvents in S. A. Adelman, Int. J. Quantum Chem. Symp. **21**, 199 (1987).

[6] (a) For applications to vibrational energy relaxation in monatomic liquids, see S. A. Adelman and R. H. Stote, J. Chem. Phys. **88**, 4397 (1988); R. H. Stote and S. A. Adelman, *ibid.* **88**, 4415 (1988). (b) For a "molecular derivation" of the isolated binary collision model based on the techniques of Ref. 6(a), see S. A. Adelman, R. Muralidhar, and R. H. Stote, J. Chem. Phys. (in press). (c) For an extension to vibrational energy relaxation in molecular liquids, see S. A. Adelman, R. Muralidhar, and R. H. Stote (unpublished). (d) Also see S. E. Huston, P. J. Rossky, and D. A. Zichi, J. Am. Chem. Soc. **111**, 5680 (1989), and references therein.

[7] (a) A brief synopsis is given in S. A. Adelman, J. Mol. Liquids **39**, 265 (1988). (b) For a more recent review, see F. Patron and S. A. Adelman, Chem. Phys. **152**, 121 (1991).

[8] (a) J. P. Bergsma, B. J. Gertner, K. R. Wilson, and J. T. Hynes, J. Chem. Phys. **86**, 1356 (1987). The analysis in Sec. III of the present paper was suggested by a discussion in this reference. (b) B. J. Gertner, K. R. Wilson, and J. T. Hynes, J. Chem. Phys. **90**, 3537 (1989). (c) B. J. Gertner, J. P. Bergsma, K. R. Wilson, S. Lee, and J. T. Hynes, J. Chem. Phys. **86**, 1377 (1987).

[9] See, for example, I. Benjamin and K. R. Wilson, J. Chem. Phys. **90**, 4176 (1989); J. P. Bergsma, J. R. Reimers, K. R. Wilson, and J. T. Hynes, *ibid.* **85**, 5625 (1986); J. P. Bergsma, P. M. Edelsten, B. J. Gertner, K. R. Huber, J. R. Reimers, K. R. Wilson, and S. M. Wu, Chem. Phys. Lett. **123**, 394 (1986).

[10] A dynamical cage effect was recently *observed in the* $Mn_2(CO)_{10} \rightarrow 2MnCO_5$ photolysis reaction [K. Nelson (private communication)].

[11] See, for example, R. D. Levine and R. B. Bernstein, *Molecular Reaction Dynamics and Chemical Reactivity* (Oxford University, New York, 1989); J. I. Steinfeld, J. S. Francisco, and W. L. Hase, *Chemical Kinetics and Dynamics*, (Prentice-Hall, Englewood Cliffs, 1989).

[12] A separable reaction coordinate departing from the transition state of a typical 1 eV activation-barrier potential-energy surface in the gas phase will accelerate to 8.4 times the mean thermal velocity in ~1/4 to 1/8 of a molecular diameter. An automobile subject to a suitably scaled up acceleration would increase its speed from 65 to 540 miles per hour over a distance scale of ~1–2 yards.

[13] See, for example, M. Berkowitz and W. Wan, J. Chem. Phys. **86**, 376 (1987).

[14] See, for example, C. K. Ingold, *Structure and Mechanism in Organic Chemistry*, 2nd ed. (Harper and Row, New York, 1981).

[15] (a) S. Chandrasekhar, Rev. Mod. Phys. **15**, 1 (1943). (b) H. A. Kramers, Physica (Utrecht) **7**, 284 (1940).

[16] The "frozen-solvent" limit, referred to as the "Einstein limit" in Ref. 1(a), has been discussed for some time in the proton transfer literature. (a) For qualitative discussions, see, for example, E. Grunwald and E. Price, J. Am. Chem. Soc. **86**, 2970 (1964); E. Grunwald, Prog. Phys. Org. Chem. **3**, 317 (1965); M. M. Kreevoy and R. A. Kretchmer, J. Am. Chem. Soc. **86**, 2435 (1964); R. P. Bell, Discuss Faraday Soc. **39**, 16 (1965); J. M. Williams and M. M. Kreevoy, Adv. Phys. Org. Chem. **6**, 63 (1968). (b) For a quantitative discussion, see J. L. Kurz and L. C. Kurz, J. Am. Chem. Soc. **94**, 4451 (1972).

[17] (a) J. Chandrasekhar, S. F. Smith, and W. L. Jorgensen, J. Am. Chem. Soc. **107**, 154 (1985); (b) J. Chandrasekhar and W. L. Jorgensen, *ibid.* **107**, 2974 (1985).

[18] R. F. Grote and J. T. Hynes, J. Chem. Phys. **73**, 2715 (1980). See also, for example, J. T. Hynes, J. Stat. Phys. **42**, 149 (1986), and references therein; S. Lee and J. T. Hynes, Chem. Phys. **88**, 6853 (1988).

[19] (a) G. van der Zwan and J. T. Hynes, J. Chem. Phys. **76**, 2993 (1982); **78**, 4174 (1988); (b) Chem. Phys. **90**, 21 (1984).

[20] Gertner *et al.* (Ref. 8) actually define $r_{as} = -(1/2)r_c$.

[21] See, for example, J. C. Keck, Discuss. Faraday Soc. **33**, 173 (1962).

[22] See, for example, P. Peckukas and F. J. McLafferty, J. Chem. Phys. **58**, 1622 (1973); W. H. Miller, *ibid.* **61**, 1823 (1974).

[23] See, for example, D. G. Truhlar and B. C. Garrett, Acc. Chem. Res. **13**, 440 (1980).

[24] We utilize the term "zeroth order" since the solute potential-energy surface cannot be specified exactly in the liquid because of the effects of fluctuations and energy dissipation.

[25] Equations (2.6) are a refined version of equation of motion derived in Ref. 5. In Eqs. (2.6) the approximation $\langle \partial F/\partial y \rangle_0 \ll \partial \langle F \rangle_0/\partial y$ utilized in Ref. 5 is lifted.

[26] *Classical Fluids*, edited by H. L. Frisch and J. L. Lebowitz (Benjamin, New York, 1964).

[27] L. J. Lowden and D. Chandler, J. Chem. Phys. **61**, 5228 (1974); see also, for example, F. Hirata, B. M. Pettitt, and P. J. Rossky, *ibid.* **77**, 509 (1982).

[28] We assume macroscopically isotropic liquids.

[29] In this paper we implicitly assume that the solute z coordinates as well as the q coordinates remain nearly "frozen" in the early-time regime. This assumption may not be realistic for high-frequency solute vibrational motions.

[30] R. A. Marcus, J. Chem. Phys. **45**, 4493 (1966); **45**, 4500 (1966); **49**, 2610 (1968).

[31] W. H. Miller, N. C. Handy, and J. E. Adams, J. Chem. Phys. **72**, 99 (1980).

[32] This holds only if there is a one-to-one correspondence between fluctuating forces $\tilde{F}$ and environmental configurations zq.

[33] This is only true if $\Omega_0^2 > 0$.

[34] R. A. Marcus, J. Chem. Phys. **24**, 966 (1956).

[35] Equation (4.2) corrects an error in Eq. (5) of Ref. 17(a).

[36] Here and below we denote the Laplace transform $\mathcal{L}$ of an arbitrary function of time $f(t)$ by $\hat{f}(z)$.